AMERICAN SOCIETY FOR MICROBIOLOGY | Journal of Virology®

GENOME REPLICATION AND REGULATION OF VIRAL GENE EXPRESSION

The ORF45 Protein of Kaposi Sarcoma-Associated Herpesvirus Is an Inhibitor of p53 Signaling during Viral Reactivation

Dina Alzhanova,[a] James O. Meyo,[a] Angelica Juarez,[a] Dirk P. Dittmer[a]

[a]Department of Microbiology and Immunology, Lineberger Comprehensive Cancer Center, The University of North Carolina at Chapel Hill, Chapel Hill, North Carolina, USA

ABSTRACT Kaposi sarcoma-associated herpesvirus (KSHV) is a carcinogenic double-stranded DNA virus and the etiological agent of Kaposi sarcoma (KS), primary effusion lymphoma (PEL), and multicentric Castleman's disease (MCD). To prevent premature apoptosis and support its replication cycle, KSHV expresses a series of open reading frames (ORFs) that regulate signaling by the p53 tumor suppressor protein. Here, we describe a novel viral inhibitor of p53 encoded by KSHV ORF45 and identify its mechanism of action. ORF45 binds to p53 and prevents its interactions with USP7, a p53 deubiquitinase. This results in decreased p53 accumulation, localization of p53 to the cytoplasm, and diminished transcriptional activity.

IMPORTANCE Unlike in other cancers, the tumor suppressor protein p53 is rarely mutated in Kaposi sarcoma (KS). Rather, Kaposi sarcoma-associated herpesvirus (KSHV) inactivates p53 through multiple viral proteins. One possible therapeutic approach to KS is the activation of p53, which would result in apoptosis and tumor regression. In this regard, it is important to understand all the mechanisms used by KSHV to modulate p53 signaling. This work describes a novel inhibitor of p53 signaling and a potential drug target, ORF45, and identifies the mechanisms of its action.

KEYWORDS KSHV, lytic, ORF45, p53, TP53, USP7, HAUSP, primary effusion lymphoma, PEL, ubiquitination

Kaposi Sarcoma-associated herpesvirus (KSHV), also known as human herpesvirus 8 (HHV8), is a double-stranded DNA virus that is linked to several malignancies, including Kaposi sarcoma (KS), primary effusion lymphoma (PEL), and the plasmablastic form of multicentric Castleman's disease (MCD). KSHV is necessary, but not sufficient, for tumor development. KSHV-associated cancers carry alterations in many cellular genes (1) but, strangely, no mutations in the p53 or Rb tumor suppressor proteins. The experiments reported here continue a long line of research (2–4) aimed at identifying interactions between viral proteins and p53.

The tumor suppressor protein p53 is a transcription factor colloquially known as the "guardian of the genome" because it plays a key regulatory role in the maintenance of genomic stability. It is involved in multiple processes, including cell cycle arrest, DNA repair, apoptosis, cellular senescence, and cell differentiation, as well as innate immunity, including to DNA viruses, which deposit foreign DNA into the nucleus (reviewed in reference 5). The p53 protein levels are controlled by multiple mechanisms, including its interactions with E3 ubiquitin-protein ligases, mainly human double minute 2 (HDM2), and the corresponding deubiquitinating enzymes, such as ubiquitin-specific-processing protease 7 (USP7), also called herpesvirus-associated ubiquitin-specific protease (HAUSP), as reviewed previously (6). USP7 binds p53 and HDM2 in a mutually exclusive manner (7, 8). Under normal conditions, USP7 is preferentially bound to HDM2 via the death domain-associated protein DAXX, which prevents self-ubiquitination of HDM2 and leads to HDM2 accumulation and consequent downregulation of p53 (9). In response to DNA damage, DNA

Citation Alzhanova D, Meyo JO, Juarez A, Dittmer DP. 2021. The ORF45 protein of Kaposi sarcoma-associated herpesvirus is an inhibitor of p53 signaling during viral reactivation. J Virol 95:e01459-21. https://doi.org/10.1128/JVI.01459-21.

Editor Felicia Goodrum, University of Arizona

Address correspondence to Dirk P. Dittmer, dittmer@med.unc.edu.

Received 1 September 2021
Accepted 9 September 2021
Accepted manuscript posted online 15 September 2021
Published 9 November 2021

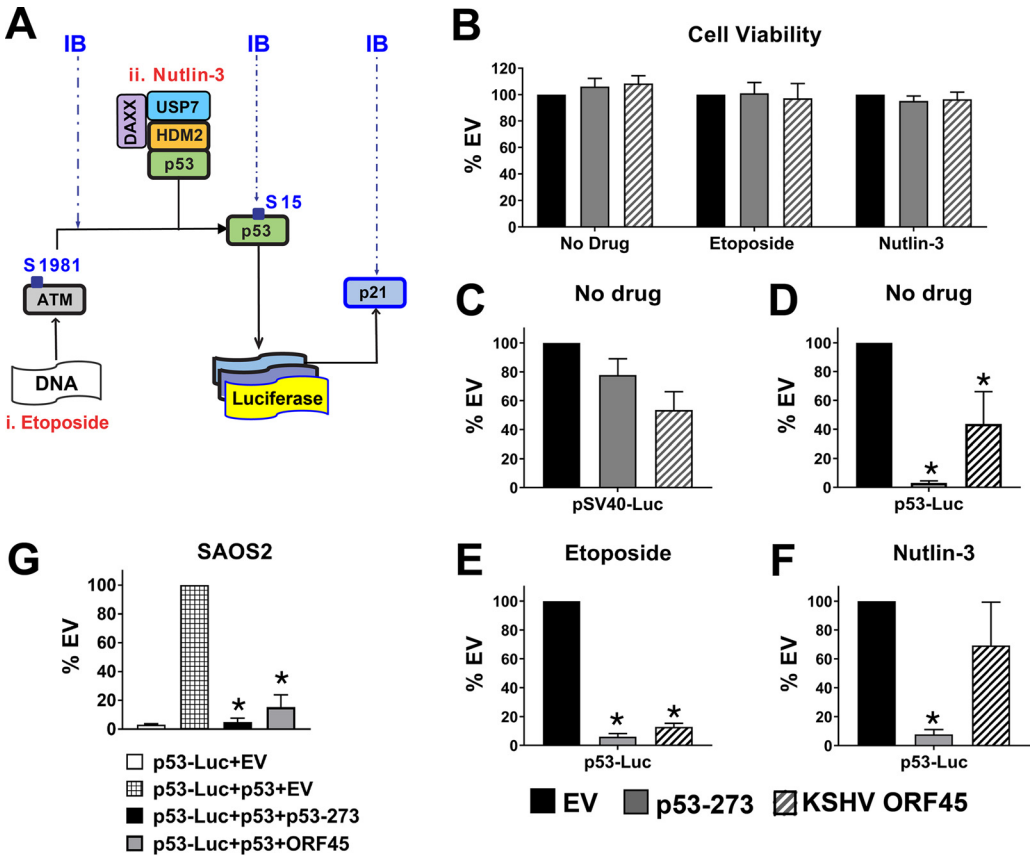

FIG 1 p53-luciferase (Luc) screening of virus-encoded open reading frames (ORFs). (A) p53 signaling is activated either by etoposide that binds and inhibits topoisomerase II, which results in the formation of double-strand breaks (DSB) and activates the DNA damage response (DDR), or by nutlin-3, which inhibits MDM2 binding to p53 and results in p53 activation. ATM senses DSB, autophosphorylates, and phosphorylates p53 and HDM2 (an E3 ubiquitin ligase), which breaks the HDM2-USP7-DAXX complex, promotes binding of USP7 to p53, and rescues p53 accumulation. HDM2 self-ubiquitinates and gets degraded via proteasomal pathway. As a result, p53 target genes, including cell cycle kinase (CDK) inhibitor p21, are expressed. The response is measured using a Luc reporter assay and immunoblotting with antibodies (Abs) specific for ATM pSer1981, ATR pThr1989, p53 pSer15, p53, and p21. (B) Cell viability for empty vector (EV) (pCMV-Neo-Bam), p53-273 (pCMV-Neo-Bam-*p53*R273H), or ORF45-Flag was measured with the CellTiter-Glo luminescent cell viability assay kit following transfection with each vector (18 h), treatment with indicated drugs (6 h), and an additional 24 h-incubation. (C to F) p53-Luc assays for KSHV ORF45-expressing cells, untreated or stimulated with etoposide or nutlin-3. U2OS cells were transfected with either pGL3 control reporter (C) or p53-responsive reporter pGL13 (D to F) and EV or plasmids expressing *p53*R273 or ORF45-Flag. At 18 h posttransfection (p.t.), the cells were stimulated with 5 μM etoposide (E) or 10 μM nutlin-3 (F) for 6 h or left untreated (C and D) and then incubated for 24 h. (G) p53-Luc assay for KSHV ORF45-expressing SAOS-2 (p53-null) cells. The cells were transiently transfected with p53-Luc reporter alone or with wild-type p53 and either EV, *p53*R273, or ORF45-Flag expression vectors. Firefly luciferase levels were measured with the One-Glo luciferase assay system. *P* values were calculated for comparison to the empty vector using Student's *t* test ($n = 4$) and are indicated with an asterisk (*) at the stringent $P \leq 0.001$ level to account for multiple comparisons.

damage-sensing kinases, ataxia telangiectasia mutated kinase (ATM), Rad3-related kinase (ATR), and DNA protein kinase (DNA-PK) phosphorylate HDM2 and p53. This first leads to the dissociation of HDM2 from its complex with USP7 and DAXX, causing subsequent HDM2 self-ubiquitination and degradation, and second, promotes the binding of USP7 to p53 directly. The net result is p53 accumulation, nuclear translocation, and transcription of p53-target genes, including the cell cycle kinase (CDK) inhibitor p21 (Fig. 1A). Additionally, ATM activation induces USP7 dephosphorylation by ATM-dependent PPM1G phosphatase, which contributes to dissociation of the HDM2-DAXX-USP7 complex (10). In summary, the precise regulation of ubiquitination is central to the activation of p53.

Like cancers associated with other DNA tumor viruses, KSHV-driven cancers typically express wild-type (WT) p53 and possess functional DNA damage-induced p53 signaling (3). This may explain the substantial clinical response rates of KS to DNA-damaging

agents such as oral etoposide, bleomycin, and intravenous doxorubicin (11, 12). Activating wild-type p53 has been proposed as a therapeutic modality for KS (2), but this has not yet progressed to clinical studies. Like other DNA tumor viruses, KSHV directly controls p53 activity, presumably for the benefit of viral replication and for the establishment of latency. The control of p53 protein levels by KSHV is multifaceted and involves multiple viral open reading frames (ORFs) that modulate p53 signaling. KSHV undergoes multiple stages during infection, including entry, latency, reactivation, and replication; therefore, it would be consistent for this virus to evolve multiple means of interfering with p53 signaling, each specific to one particular stage of the viral life cycle and each using a different viral protein.

Four p53-inhibitory KSHV proteins were previously identified and studied because of their role in the latent phase of the viral life cycle. They are the latency-associated nuclear antigen (LANA; ORF73) and the viral interferon regulatory factors (vIRF) vIRF-1, vIRF-3 (LANA-2), and vIRF-4. LANA, vIRF-1, and vIRF-3 bind p53 directly (4, 13–17). The vIRF1, in addition, inactivates ATM (14), and vIRF4 stabilizes HDM2, which increases p53 degradation (18). These proteins were also shown to interact with the p53 deubiquitinase USP7 (19–22). Clearly, some or all the KSHV latent proteins are also expressed during lytic replication. The vIRF-1 protein, for instance, is induced upon reactivation (23, 24); however, it is not known if exclusively lytic KSHV proteins or tegument components also impinge on p53 signaling. One could envision that tegument proteins are needed to counteract p53 activation prior to immediate early viral gene expression and that lytic KSHV proteins block additional activities of p53 signaling or simply augment the activities of LANA and the vIRFs in the face of high levels of activated p53.

To extend this prior work, we explored the possible mechanisms of KSHV-p53 interactions during the lytic phase of the virus. A large-scale screen for viral interactors of p53 identified KSHV ORF10 and ORF45 as potential hits. This initial screen and the mechanism of the ORF10-p53 interaction were reported recently (25). ORF45 had been shown to bind USP7 (26), but the connection between that interaction and p53 function had not been drawn previously. Here, we demonstrate first that ORF45 binding to USP7 redirects its deubiquitinating activity away from p53. Therefore, p53 ubiquitination levels are increased and overall p53 protein levels are decreased. Second, we demonstrate that ORF45 binds p53 directly, which localizes p53 to the cytoplasm, thereby inhibiting its nuclear transcriptional transactivation function. The net effect of these different mechanisms is complete inactivation of p53 (and inhibition of p53-dependent apoptosis) at a time in the viral life cycle at which the KSHV DNA genome replicates and accumulates free DNA ends and recombination products in the host cell nucleus.

RESULTS

ORF45 inhibits the transcriptional transactivation function of p53. ORF45 was recovered as a potential hit in a high-throughput screen for viral interactors of p53 (25). To validate the result of this ectopic expression screen, potential cytotoxicity due to overexpression was ascertained using a cell viability assay in the presence or absence of the drug (Fig. 1B). No evidence for toxicity compared to that of the empty vector control was detected. To rule out nonspecific inhibition of basal promoter activity, a plasmid expressing luciferase (Luc) under the minimal SV40 promoter was tested (Fig. 1C). ORF45 did not influence basal promoter activity. Next, ORF45 activity on a p53-responsive promoter was compared between untreated or etoposide-treated U2OS cells. U2OS cells carry wild-type p53, which is inducible by etoposide. As a positive control, a plasmid expressing the dominant negative p53 R273H mutant (27, 28), referred to as p53-273, was used. ORF45 inhibited p53-dependent luciferase expression in untreated cells to 44% that of empty vector (EV) (Fig. 1D). However, in etoposide-treated cells, the inhibition was significantly more efficient (13% of EV) and was comparable to that for the dominant negative mutant p53-273 (6% of EV; Fig. 1E).

To identify the stage at which the p53 signaling cascade was inhibited, U2OS cells were stimulated with nutlin-3, a small-molecule inhibitor that binds to HDM2,

interferes with HDM2-p53 interactions, and thereby activates p53 independently of DNA damage (29). ORF45 interfered with nutlin-3-induced activation of the p53-responsive transcriptional reporter as well, but not nearly as efficiently as the p53-273 mutant allele (66% of EV; Fig. 1F), which is a dominant negative DNA contact mutant that forms a poisoned tetramer (30, 31).

Finally, ORF45-mediated inhibition of p53 transcriptional transactivation was recapitulated in p53-null SAOS2 cells (32). The cells were cotransfected with either p53-Luc reporter alone or with wild-type (WT) p53 and either EV, p53-273, or ORF45 expression vectors. Similarly to those in etoposide-treated U2OS cells, p53-Luc levels induced by ectopic p53 in SAOS-2 cells were significantly inhibited by both the p53-273 mutant control and ORF45 (5% and 15% of EV, respectively; Fig. 1E).

ORF45 increases p53 ubiquitination and degradation through binding to USP7. ORF45 was recently reported to interact with USP7 and to sequester USP7 in the cytoplasm (26). As USP7 is a p53 deubiquitinase, we hypothesized that ORF45 downregulates p53 signaling by inhibiting p53 deubiquitination through USP7. An amino acid sequence analysis of ORF45 revealed several potential USP7-binding motifs (P/AxxS; Fig. 2A). One of these motifs, "EGPS" at amino acid position 223 to 226, was also observed in the KSHV vIRF-1 and vIRF-3 proteins, as well as the in the Epstein-Barr Virus nuclear antigen 1 (EBNA1) protein (20, 21, 33). Mutation of the KSHV ORF45 EGPS motif was shown to abrogate the ORF45-USP7 protein-protein interaction and to restore the nuclear localization of USP7 (26).

To independently confirm the ORF45-USP7 interaction, constructs that expressed ORF45 tagged with C-terminal 3×Flag epitope and that were either wild type or carried the E223A-S226A mutation were transiently transfected into U2OS cells. Wild-type ORF45-Flag bound to anti-Flag beads coimmunoprecipitated with USP7 (Fig. 2B). It retained USP7 in the cytoplasm in untreated and etoposide-stimulated cells (Fig. 2C and D, arrows). The ORF45$^{E223A\text{-}S226A}$ mutation significantly affected the ORF45-USP7 interactions, as shown by reduced levels of coimmunoprecipitated USP7 protein (Fig. 2B), and it allowed USP7 nuclear localization in untreated or etoposide-stimulated cells (Fig. 2E and F, arrows).

Next, p53 ubiquitination in the presence of the wild-type ORF45 and the ORF45 $^{E223A\text{-}S226A}$ mutant was evaluated. Expression of the wild-type ORF45 increased p53 ubiquitination levels compared to those in a mock-transfected control, as judged by the abundance of ubiquitinated p53 species migrating above 250 kDa (Fig. 2G, arrow). Conversely, ORF45 $^{E223A\text{-}S226A}$ mutant reduced p53 ubiquitination levels compared to those of the wild-type ORF45 (Fig. 2G). These results suggest that ORF45 affects p53 ubiquitination by interacting with USP7 and redirecting its deubiquitination activity away from p53 and, presumably, toward KSHV ORF33.

ORF45 also inhibits p53 transcriptional activity independently of USP7. To further investigate the mechanisms of p53 downregulation by ORF45 and assess the effect of disruption of ORF45-USP7 interactions on p53 activity, the accumulation of the following major protein components of p53 signaling were evaluated: (i) p53, total and phosphorylated at Ser-15 (an established indicator of p53 activation by the DNA damage response [DDR], referred to as p53-pS15 [34, 35]); (ii) p53 target protein p21; and (iii) HDM2, whose expression is positively regulated by p53 via a negative feedback loop; a kinase activated by ATM kinase, total or phosphorylated at S1981. U2OS cells were transfected with either empty vector (EV) control, pcDNA3.1-ORF45-Flag, or pcDNA-ORF45$^{E223A\text{-}S226A}$-Flag plasmids or left untreated for 18 h and then incubated with 10 μM etoposide for 6 h (Fig. 3). The cell lysates were analyzed by SDS-PAGE and immunoblotting. Wild-type ORF45 and ORF45$^{E223A\text{-}S226A}$ proteins were readily expressed, migrated at the described molecular weight (~78 kDa [36]) and accumulated to similar levels.

Wild-type ORF45 reduced the levels of total and phosphorylated p53, as well as those of p21, compared to those with EV (Fig. 3A). Reduction in total p53 accumulation was reproduced in a cycloheximide chase experiment, for which expression of p53 in U2OS cells was stimulated with etoposide for 1.5 h and then chased in the presence of cycloheximide for 2 h. Unlike in untransfected control cells, p53 levels were virtually

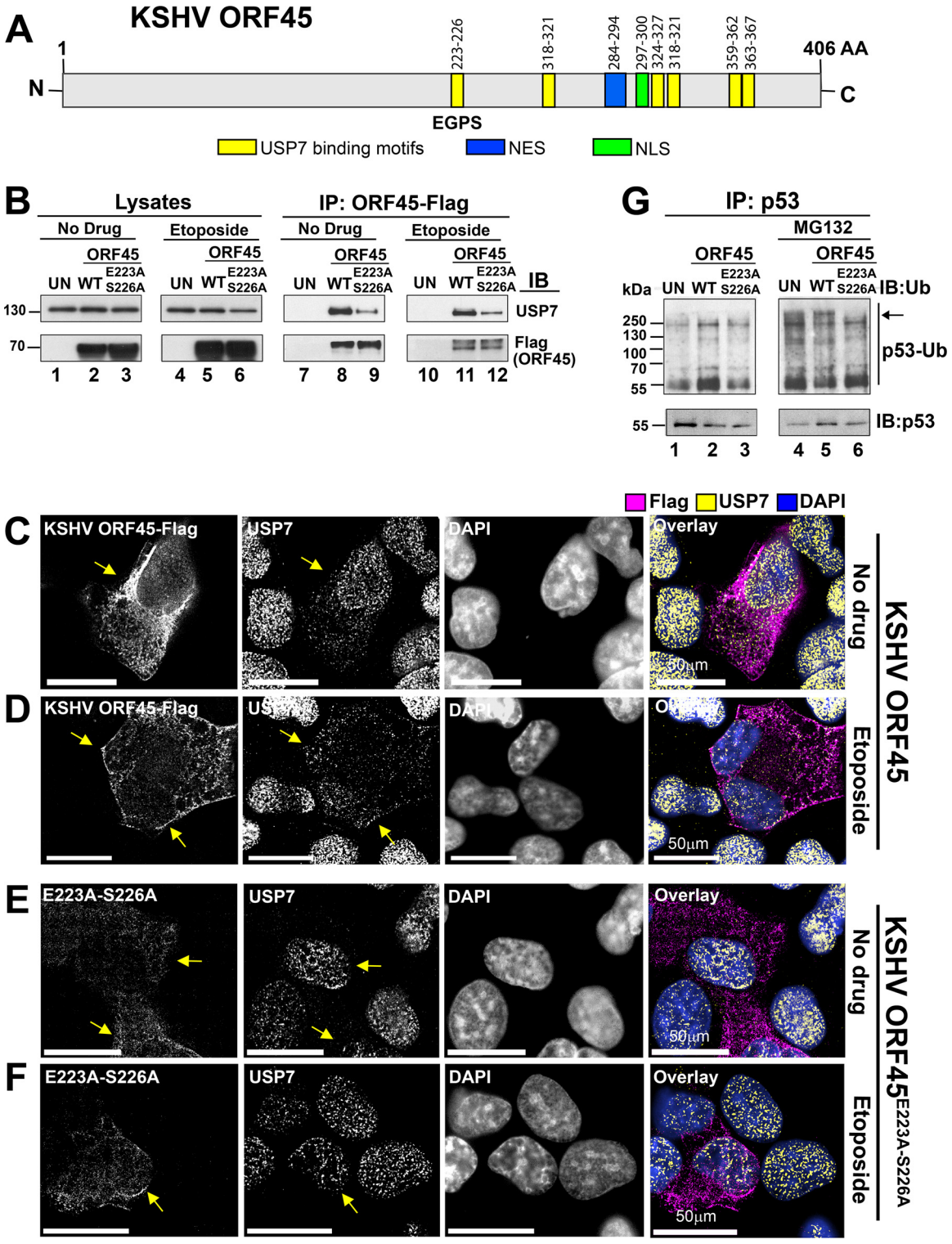

FIG 2 ORF45 interacts with USP7. (A) Schematic depiction of ORF45 amino acid sequence. The protein possesses multiple predicted USP7 binding motifs (yellow boxes), a single nuclear localization signal (NLS; green box), and two nuclear export signal (NES; blue boxes) motifs. (B) Endogenous p53 pulldown. U2OS cells were transfected with constructs expressing either wild-type ORF45-Flag or ORF45$^{E223A-S226A}$-Flag or left untransfected (UN). At 18 h p.t., the cells were stimulated with 10 μM etoposide for 6 h. ORF45-Flag or ORF45$^{E223A-S226A}$-Flag were immunoprecipitated with mouse α-Flag Ab. Lysates and immunoprecipitants were tested with rabbit α-USP7 and mouse α-Flag Abs. (C to F) ORF45 retains USP7 in the cytoplasm. U2OS cells were transfected with constructs expressing either wild-type ORF45-Flag or ORF45$^{E223A-S226A}$-Flag. At 18 h p.t., the cells were left untreated or were stimulated with 10 μM etoposide for 1.5 h (D, F), fixed with methanol, and stained with the indicated Abs. The images were taken as Z-stack sections and subjected to a digital deconvolution. Bar, 50 μm. Arrows indicate the cell expressing KSHV ORF45 (wild-type or mutant). (G) ORF45

(Continued on next page)

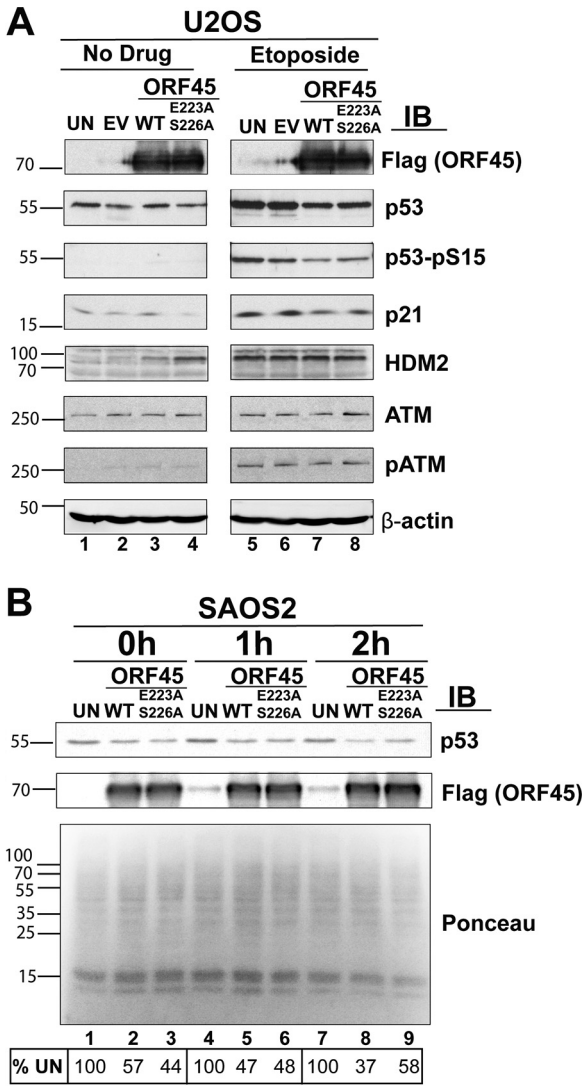

FIG 3 Expression of the p53-signaling components in the presence of ORF45. (A) Cells were transfected with empty vector (EV) or constructs expressing either wild-type ORF45-Flag or ORF45$^{E223A-S226A}$-Flag or were left untransfected (UN). At 18 h after transfection, the cells were stimulated with 10 μM etoposide for 6 h. Cell lysates were analyzed by SDS-PAGE and immunoblotting with indicated antibodies. (B) Total p53 accumulation tested by cycloheximide chase assay. U2OS cells were transfected with either wild-type ORF45-Flag or ORF45$^{E223A-S226A}$-Flag or were left untransfected (UN) were stimulated with 10 μM etoposide for 1.5 h. p53 expression was chased in the presence of 100 μg/ml cycloheximide for the indicated time periods and tested by immunoblotting.

undetectable in wild-type ORF45-expressing cells after 2 h of chasing (Fig. 3B). The phenotype was even more pronounced when evaluated using immunofluorescence. For this experiment, U2OS cells were transfected with ORF45-expressing plasmids for 18 h, then stimulated with 10 μM etoposide for 1.5 h and processed as described in Materials and Methods. The numbers and levels of p53–pS15-positive cells were drastically reduced, and p21 was virtually undetectable in wild-type ORF45-expressing cells compared to levels in the neighboring cells that did not get transfected (Fig. 4A and C, arrows; quantitation in Fig. 4E).

FIG 2 Legend (Continued)
expression, but not that of the E223A-S226A mutant, increases p53 ubiquitination. U2OS cells were transfected with constructs expressing either wild-type ORF45-Flag or ORF45$^{E223A-S226A}$-Flag or were left untransfected. At 18 h p.t., the cells were incubated in the presence or absence of 30 μM MG132 for 6 h. p53 was coimmunoprecipitated with p53-speciifc mouse pAb421 Ab and blotted with rabbit α-ubiquitin and mouse α-p53 DO7 Abs.

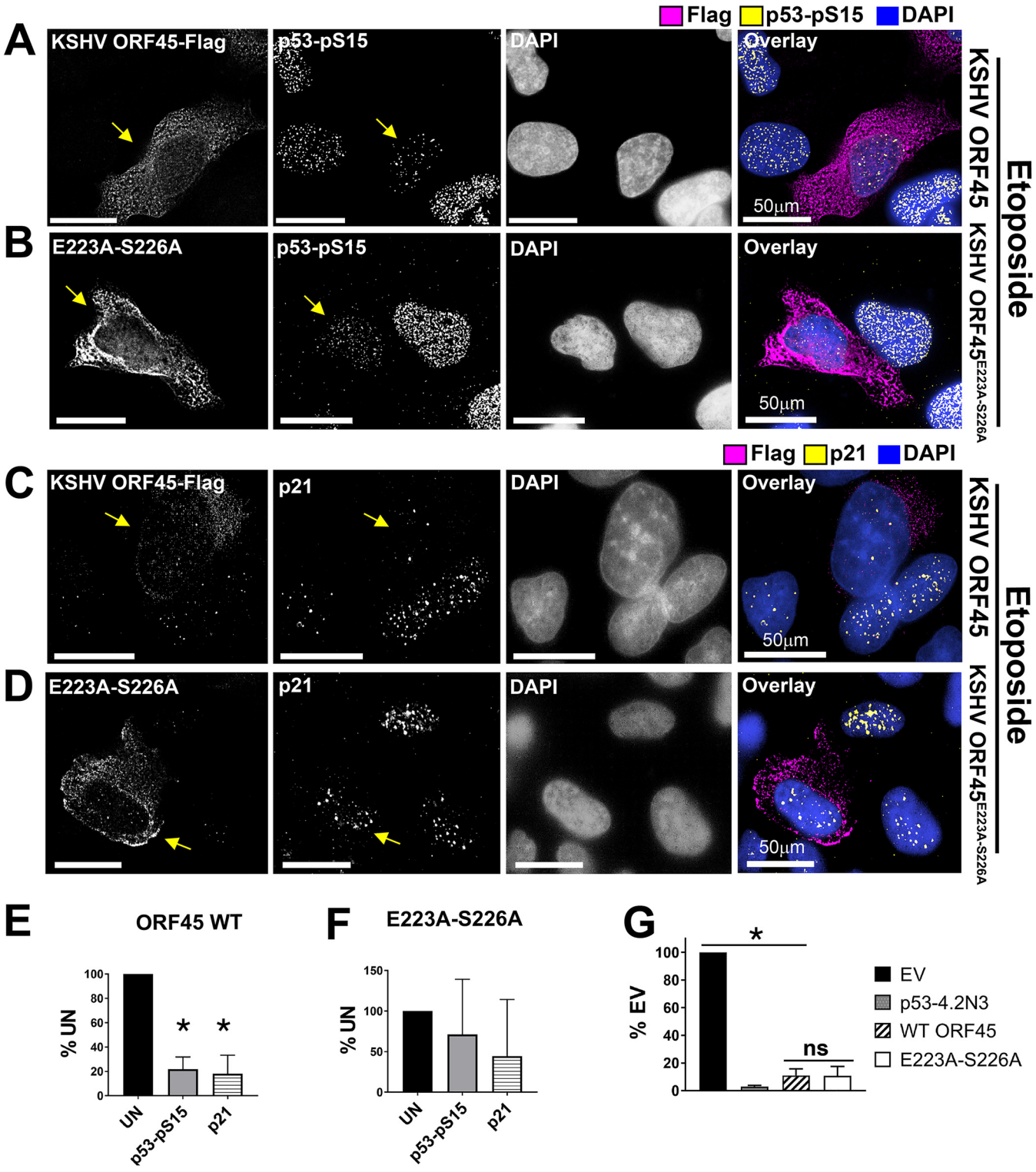

FIG 4 ORF45 inhibits accumulation of phosphorylated p53 and p21 and inhibits p53 transcriptional transactivation independently of USP7. (A to D) Accumulation of phosphorylated p53 and p21 determined by immunofluorescence (IF). U2OS cells were transfected with plasmids expressing ORF45-Flag or ORF45$^{E223A-S226A}$-Flag. At 18 h after transfection, the cells were stimulated with 10 μM etoposide for 1.5 h, fixed, and stained with anti-Flag, anti-phospho-p53Ser15, or anti-p21 antibodies. DAPI (4′,6-diamidino-2-phenylindole) was used to delineate the nucleus. The images were subjected to digital deconvolution. Each image represents an individual optical section. Bar, 50 μm. Arrows indicate cells expressing ORF45 (wild type or mutant). (E and F) Protein levels in ORF45-Flag-expressing (E) or ORF45$^{E223A-S226A}$-Flag-expressing (F) cells determined by immunofluorescence relative to levels in untransfected cells (%UN) that were calculated based on pixel density measured using ImageJ software. Bars indicate standard error of the mean (SEM) ($n \geq 8$). *P* values were calculated using Student's *t* test. ns, $P > 0.05$; *, $P \leq 0.001$. (G) p53-Luc assay for ORF45 (wild type or E223A-S226A mutant)-expressing cells stimulated with etoposide. U2OS cells were transfected with either p53-responsive reporter pGL13 and EV or plasmids expressing *p53*R273, ORF45-Flag, or ORF45$^{E223A-S226A}$-Flag. At 18 h posttransfection (p.t.), the cells were stimulated with 5 μM etoposide and then incubated for 24 h. Firefly luciferase levels were measured with the One-Glo luciferase assay system. *P* values were calculated using Student's *t* test ($n = 4$). ns, $P > 0.05$; *, $P \leq 0.001$.

The ORF45 $^{E223A-S226A}$ mutation partially rescued expression of total p53, p53-pS15, and p21 upon etoposide stimulation as shown by immunoblotting (Fig. 3A), cycloheximide chase for total p53 (Fig. 3B), and immunofluorescence experiments (Fig. 4B and D, arrows; quantitation in Fig. 4F); however, p53 transcriptional activity as quantitatively assessed by p53-Luc assay was not rescued (Fig. 4G). This indicated that ORF45 might use additional unidentified mechanisms to interfere with p53 function.

To exclude the possibility that ORF45 impacted p53 activation earlier in the pathway, ATM levels were evaluated. The accumulation of total and phosphorylated ATM was not affected by wild-type ORF45, nor by the ORF45$^{E223A-S226A}$ mutant, suggesting that ORF45 does not inhibit DDR driven by ATM (Fig. 3A).

Another possible mechanism for interference with p53 function would be the modulation of HDM2 function. HDM2/MDM2 was discovered as a suppressor of p53 (37). Because p53 expression itself is regulated by a positive feedback loop and because HDM2 is also a transcriptional target of p53, HDM2 typically accumulates in p53 wild-type cells stimulated with etoposide but not in untreated cells. In untreated U2OS cells expressing wild-type ORF45, HDM2 levels were higher than those in the EV control (Fig. 3A, lanes 2 and 3). Because p53 levels did not increase, as the cells were not treated with etoposide, this suggests that ORF45 may regulate HDM2 expression independently of p53. HDM2 levels were upregulated even further in the presence of the ORF45$^{E223A-S226A}$ mutant (Fig. 3A, lane 4), which does not bind to USP7 and therefore does not interfere with HDM2-USP7 interactions and negative feedback loop. Thus, ORF45 also contributes to deubiquitination and accumulation of HDM2.

ORF45 binds to p53. Because some viral p53 inhibitors have been shown to function by preventing nuclear accumulation of p53, we examined p53 subcellular localization in cells transiently transfected by ORF45 expression vectors using immunofluorescence. The p53 colocalized mostly to the cytosol in the presence of wild-type ORF45, irrespective of whether the cells were mock-treated or stimulated with etoposide (Fig. 5A and B, arrows; quantitation in Fig. 5E). This is consistent with the hypothesis that ORF45 sequesters p53 in the cytoplasm. ORF45$^{E223A-S226A}$ restored nuclear localization of p53 (Fig. 5C and D, arrows; quantitation in Fig. 5E).

The significant overlap in fluorescence signals for wild-type ORF45, the E223A-S226A mutant, and p53 confirmed their colocalization and pointed to a potential direct interaction between ORF45 and p53 independent of USP7. To test this hypothesis, a series of coimmunoprecipitation experiments were conducted. First, we used Flag antibody (Ab) to pull down ORF45-Flag and ORF45$^{E223A-S226A}$-Flag protein fusions and probed with anti-p53 antibody. p53 coimmunoprecipitated with the wild-type ORF45 and ORF45$^{E223A-S226A}$, suggesting that ORF45 interacts with p53 independently of USP7 (Fig. 6A). Second, p53 was pulled down with (i) α-p53 pab421, (ii) a nanobody binding to the p53 N terminus, or (iii) a nanobody binding to the p53 C terminus. In each case, the wild-type and the mutant ORF45 were coimmunoprecipitated (Fig. 6B and C). Next, we tested ORF45 and p53 interactions in p53-null SAOS-2 cells. For this, the cells were transfected with vectors expressing the p53-273 mutant rather than wild-type p53 to avoid induction of cell death and ORF45. Both wild-type ORF45 and the E223A-S226A mutant coimmunoprecipitated with p53 N terminus-binding nanobody (Fig. 6D). These experiments establish that ORF45 binds to p53 directly or via an adaptor protein.

Finally, the ORF45-p53 interactions were confirmed in a biologically relevant cell line. The body- and cavity-based lymphoma (BCBL1) cell line was derived from a primary effusion lymphoma (PEL) carrying the complete and replication-competent KSHV genome (38). The TREx BCBL1-RTA cell line is a derivative in which the KSHV immediate early transactivator ORF50/RTA can be induced by adding doxycycline (23). RTA in turn induces the viral lytic life cycle, and with it ORF45 expression. Confirming the experiments with transiently transfected U2OS cells, immunoprecipitation of ORF45 with α-ORF45 Ab pulled down p53, as well as USP7 (Fig. 6E, lane 3). Hence, these three proteins interact under physiological conditions in the context of the viral life cycle.

There was a limitation to this experiment, as native, untagged USP7 nonspecifically sticks to protein A/G-agarose resin. Some nonspecific binding in the "agarose only"

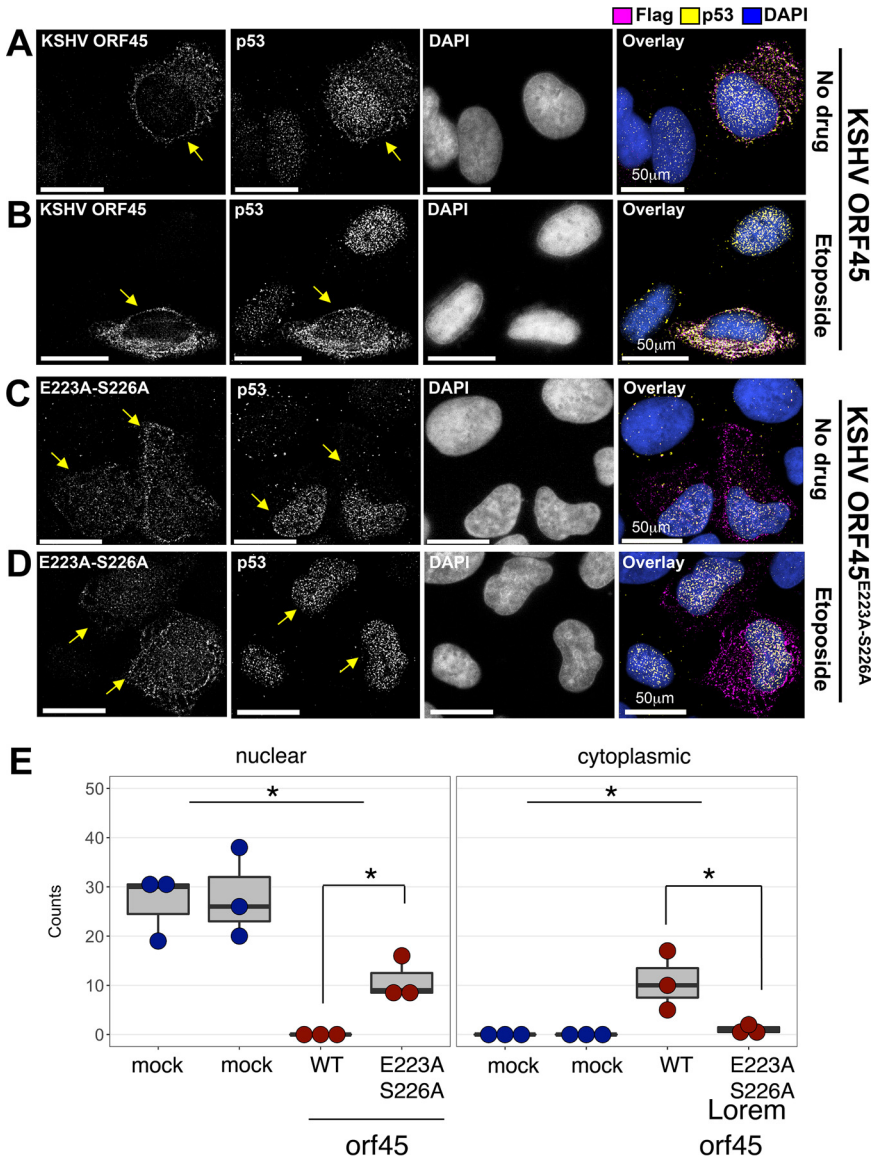

FIG 5 ORF45 sequesters p53 within the cytoplasm. (A to D) U2OS cells were transfected with plasmids expressing ORF45-Flag or ORF45$^{E223A-S226A}$-Flag. At 18 h p.t., the cells were left untreated (A and C) or were stimulated with 10 μM etoposide for 1.5 h (B and D), fixed with methanol, and stained with the indicated Abs. The images were taken as Z-stack sections and subjected to digital deconvolution. Bar, 50 μm. Arrows indicate cells expressing the ORF45 wild type or the mutant. (E) Number of cells with nuclear ("N") or cytoplasmic ("C"; the majority of the signal localizes in the cytoplasm, but residual amounts of p53 can be detectable in the nucleus) p53 localization for untransfected and cells expressing either wild-type ORF45-Flag (E) or ORF45$^{E223A-S226A}$-Flag (F), determined by immunofluorescence. Boxes indicate the interquantile range and lines the median (n = 3). P values were calculated using nonparametric factorial analysis of variance (ANOVA) following by *post hoc* pairwise comparisons using Dunnett's adjustment. *, $P \leq 0.05$.

control was visible (Fig. 6E, lane 2). This is in contrast with earlier experiments that used a ORF45-Flag fusion protein, Flag Ab, and Flag peptide (Fig. 6A, lanes 7 and 10). Unfortunately, TREx BCBL1-RTA cells only express untagged ORF45, and only one anti-ORF45 antibody was available. Nonspecific binding did not occur when p53 was immunoprecipitated, as the p53 N and C terminus-directed nanobodies and the negative binding control for agarose beads showed no detectable background and successfully coimmunoprecipitated ORF45 and USP7 (Fig. 6F). The reciprocal immunoprecipitation thus confirmed the direct ORF45-p53 interaction in the context of viral infection.

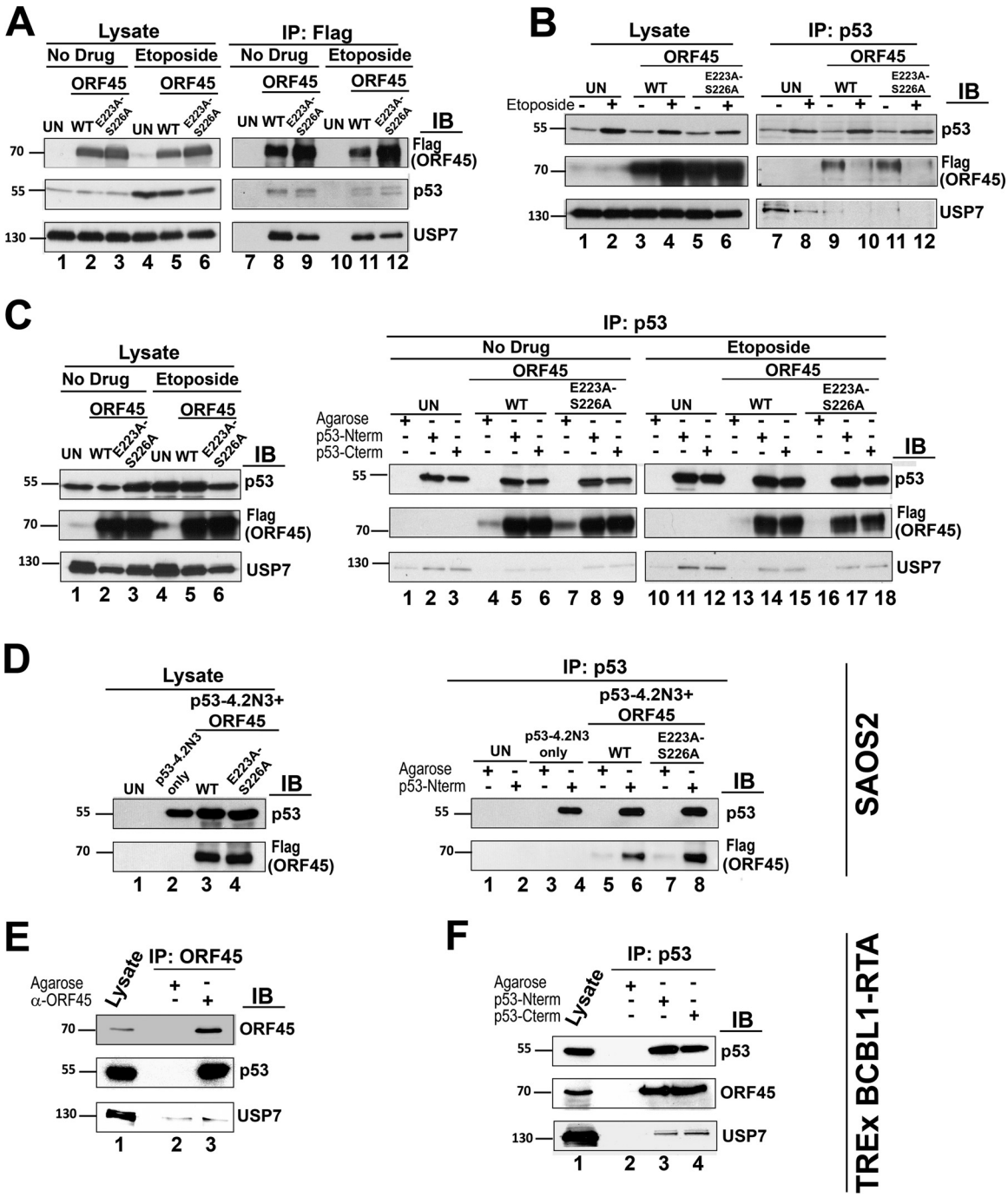

FIG 6 ORF45 binds to p53. (A) Endogenous p53 pulldown. U2OS cells were transfected with plasmids expressing ORF45-Flag or ORF45$^{E223A-S226A}$-Flag or were left untransfected (UN). At 18 h p.t., the cells were stimulated with 10 μM etoposide for 6 h. Wild-type or mutant ORF45-Flag fusions were immunoprecipitated with mouse α-Flag Ab. Lysates and immunoprecipitates were tested with mouse α-p53 DO7 and mouse α-Flag Abs. (B and C) ORF45 pulldown using p53-binding Ab. U2OS cells were transfected with plasmids expressing ORF45-Flag or ORF45$^{E223A-S226A}$-Flag or were left untransfected (UN). At 18 h p.t., the cells were stimulated with 10 μM etoposide for 6 h. p53 was immunoprecipitated with either pAb421 or the proteins binding to the p53 N or C terminus (VHH Ab). Presence of wild-type or mutant ORF45-Flag, USP7, and p53 in the lysates and immunoprecipitants was tested with mouse α-Flag and mouse α-p53 DO7 Abs. (D) Coimmunoprecipitation of ectopic p53 and ORF45 from p53-null SAOS-2 cells. Cells were transfected with vectors expressing p53-273 or ORF45 (wild type or E223A-S226A mutant). At 24 h p.t, p53 was immunoprecipitated with p53 N-terminal VHH Ab. Presence of wild-type or mutant ORF45-Flag and p53 in the lysates and immunoprecipitants was tested with mouse α-Flag and mouse α-p53 DO7 Abs. (E) p53 and USP7 coimmunoprecipitation with ORF45 from PEL-derived TREx BCBL1-RTA cells treated with 1 μg/ml doxycycline for 16 h to induce the KSHV lytic cycle. ORF45 was immunoprecipitated with α-ORF45 Ab. Presence of ORF45, p53, and USP7 was detected with mouse α-ORF45, mouse α-p53 DO7 Abs, and rabbit α-USP7 Ab, respectively. (F) ORF45 pulldown using p53-binding proteins from PEL-derived TREx BCBL1-RTA cells. The cells were treated with 1 μg/ml doxycycline for 16 h to induce the KSHV lytic cycle. p53 was immunoprecipitated with the proteins binding to the p53 N or C terminus (VHH Ab). The presence of ORF45, p53, and USP7 was detected with mouse α-ORF45, mouse α-p53 DO7 Abs, and rabbit α-USP7 Ab, respectively.

These experiments establish three novel biochemical functions for ORF45. First, ORF45 binds p53 during viral reactivation, either directly or via an adaptor protein. This binding event is independent of the ORF45-USP7 interaction, since the ORF45$^{E223A-S226A}$ mutant still immunoprecipitated p53. Second, ORF45 binding to USP7 interferes with the p53-USP7 interaction. Third, ORF45 sequesters p53 in the cytoplasm, which abrogates the transcriptional transactivation functions of p53.

ORF45 binding to p53 is sufficient to abrogate its transcriptional activity independent of cellular localization and independent of USP7. ORF45 possesses a nuclear localization signal (NLS) and a nuclear export signal (NES), which allow the protein to shuttle between the nucleus and the cytoplasm. The previously described RC ("restricted to the cytoplasm") mutation in ORF45 NLS and RN1 and RN2 ("restricted to the nucleus") mutations in ORF45 NES restrict ORF45 to the cytoplasm or the nucleus, respectively (39). To understand whether ORF45 localization plays a role in the modulation of p53 activity, the subcellular localization of p53 in the presence of ORF45^{RC}, ORF45^{RN1}, and ORF45^{RN2} mutants was examined using fluorescence microscopy either in untreated cells (low p53) or in etoposide-treated cells (high and activated p53). In untreated cells with basal levels of p53, the cytoplasm-restricted ORF45^{RC} mutant retained all p53 in the cytoplasm, where the proteins colocalized with each other. However, it did not prevent accumulation of induced and activated high levels of p53 in the nucleus upon etoposide treatment (Fig. 7A and B, arrows). Rather, some ORF45^{RC} mutant protein was dragged by p53 into the nucleus, where both proteins colocalized (Fig. 7B). In contrast, expression of ORF45^{RN1} and ORF45^{RN2} mutants resulted in accumulation and colocalization of both ORF45 and p53 in the nucleus in untreated cells and in etoposide-treated cells (Fig. 7C to F, arrows), since these mutants can never leave the nucleus and thus retain any bound p53 there as well.

Consistent with prior work in which cytoplasmic translocation of USP7 in the presence of ORF45 was blocked using leptomycin B (26), USP7 localization was nuclear in the presence of the nuclearly restricted ORF45^{RN1} and ORF45^{RN2} mutants and cytoplasmic in the presence of ORF45^{RC} (Fig. 8), i.e., the different ORF45 mutants maintained their phenotypes with regard to USP7. The three mutations that altered the subcellular localization of ORF45 had no effect on biochemical binding to p53 or USP7. All ORF45 mutants coimmunoprecipitated with p53 in untreated and etoposide-stimulated cells (Fig. 9A). Likewise, the RC, RN1, and RN2 mutations had no effect on ORF45-USP7 interactions. All ORF45 mutants coimmunoprecipitated with USP7 (Fig. 9B). All mutants inhibited p53-Luc expression as efficiently as the wild-type ORF45 (Fig. 9C). These experiments demonstrate that translocation of ORF45 between the nucleus and the cytoplasm drives the localization of both p53 and USP7, but it is dispensable for the abrogation of p53's transcriptional activity.

To assess the relative importance of ORF45-p53 and ORF45-USP7 binding on the inhibition of p53's transcriptional activity, we generated the double mutant ORF45$^{E223A-S226A/RC}$, which is deficient in binding to USP7 and is restricted to the cytoplasm, and the double mutant ORF45$^{E223A-S226A/RN2}$, which is deficient in binding to USP7 and is restricted to the nucleus. As designed, neither mutant bound USP7 (Fig. 10A) and neither mutant affected the cellular localization of USP7 (Fig. 10B to E). Both mutants still bound to p53, as shown by immunoprecipitation using p53-specific nanobodies (Fig. 11A). Next, these mutants were tested for their effect on p53-dependent transcriptional transactivation. Both mutants inhibited p53-Luc expression as efficiently as the wild-type protein (Fig. 11B), but by two different mechanisms, either by binding p53 and retaining it in the cytoplasm or by binding p53 and inhibiting its transactivation function in the nucleus. Both mechanisms were independent of USP7.

DISCUSSION

ORF45 is a large multifunctional protein encoded by KSHV that is expressed as an early gene during reactivation and that is also incorporated into virus particles (36, 40, 41). This suggests that ORF45 is present in the cell as early as initial infection, as well as when the infection switches from the latent to the lytic phase. This bimodal expression pattern correlates with the previously reported roles of ORF45 in downregulating type

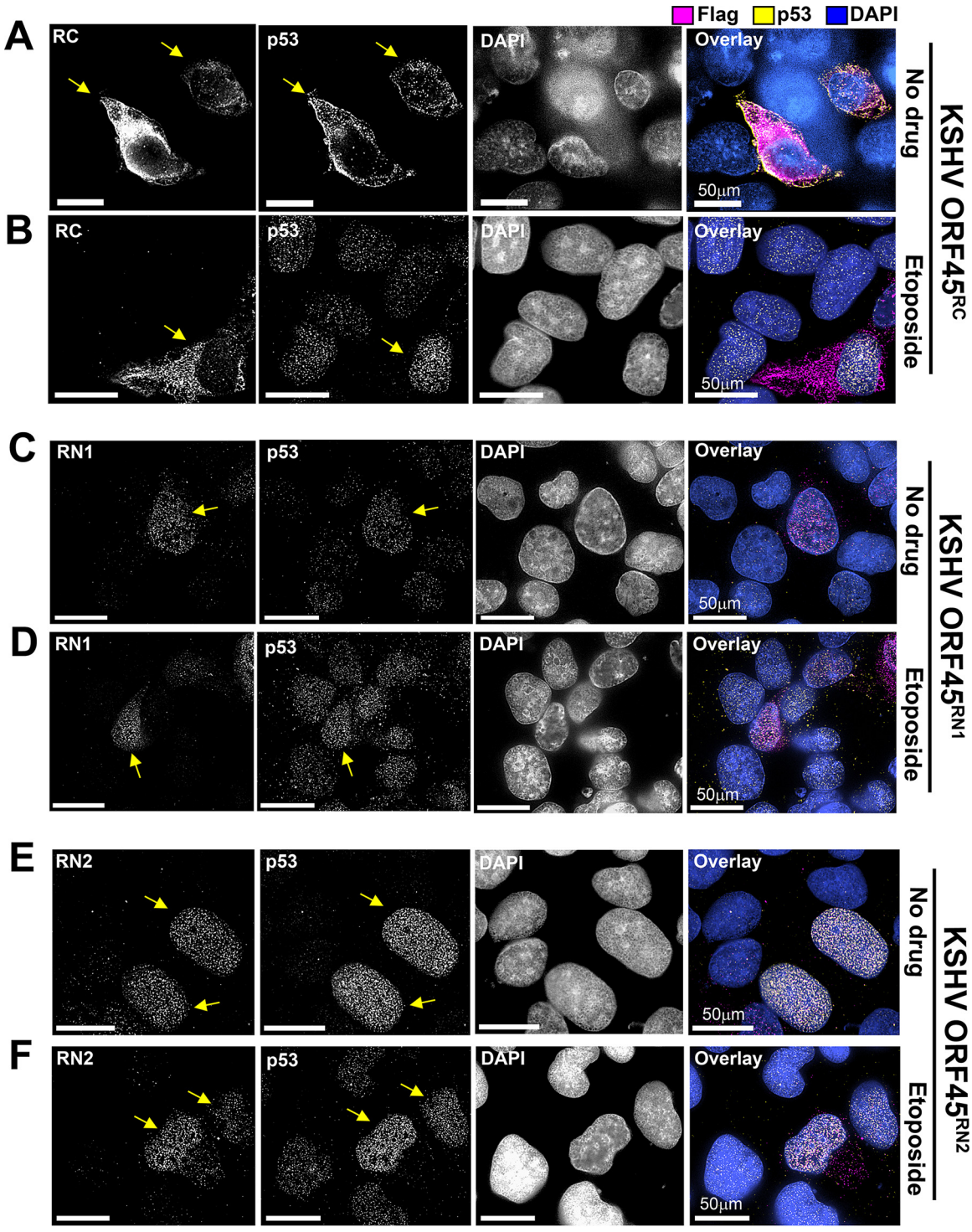

FIG 7 Shuttling of ORF45 between the nucleus and cytoplasm is required for p53 sequestration. (A to F) U2OS cells were transfected with plasmids expressing ORF45^{RC}-Flag, ORF45^{RN1}-Flag, or ORF45^{RN2}-Flag. At 18 h p.t., the cells were left untreated (A, C, E) or were stimulated with 10 μM etoposide for 1.5 h (B, D, F), fixed with methanol, and stained with the indicated Abs. The images were taken as Z-stack sections and subjected to digital deconvolution. Bar, 50 μm. Arrows indicate cells expressing the indicated ORF45 mutants.

l interferon production at early time points (42) and promoting virus maturation and egress at late time points as part of the virion assembly complex (26, 43–45).

Earlier studies have shown that ORF45 interacts with the USP7 deubiquitinase. USP7 has many targets; one of them is p53 and another one is the KSHV protein ORF33. ORF45

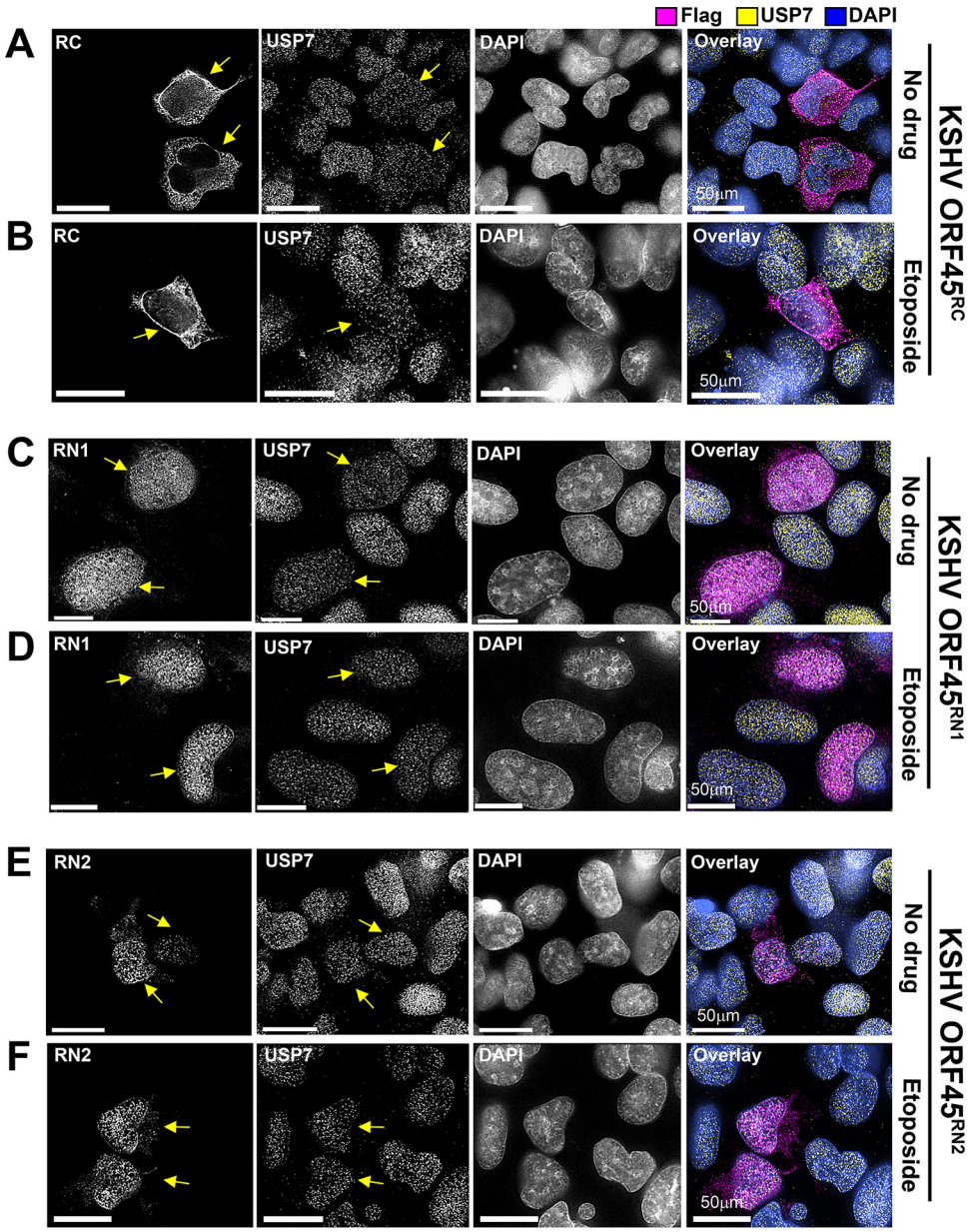

FIG 8 Shuttling of ORF45 between the nucleus and cytoplasm is required for sequestration of USP7. (A to F) U2OS cells were transfected with plasmids expressing ORF45$^{R}_{C\text{-}F}$lag, ORF45^{RN1}-Flag, or ORF45^{RN2}-Flag. At 18 h p.t., the cells were left untreated (A, C, E) or were stimulated with 10 μM etoposide for 1.5 h (B, D, F), fixed with methanol, and stained with the indicated Abs. The images were taken as Z-stack sections and subjected to digital deconvolution. Bar, 50 μm. Arrows indicate cells expressing the indicated ORF45 mutants.

facilitates the interaction between USP7 and ORF33, thereby stabilizing its expression, as USP7 deubiquitinates ORF33 and retains some ORF33 in the cytoplasm (26). Here, we found that by binding to USP7, ORF45 increased the ubiquitination of p53, resulting in p53 degradation. Whether, in addition to these two substrates, ORF45 also modulates the interaction between USP7 and other cellular substrates remains to be determined.

In addition to binding USP7, we demonstrated that ORF45 also binds directly to p53. The ORF45-p53 interaction was detectable in wild-type KSHV-infected lymphoma cells undergoing viral reactivation, i.e., under normal physiological conditions. These biochemical interactions resulted in the abrogation of p53-dependent transcriptional transactivation, and reduced the induction of total p53, Ser-15 phosphorylated p53, and p21 in response to etoposide treatment. Some of these phenotypes are the

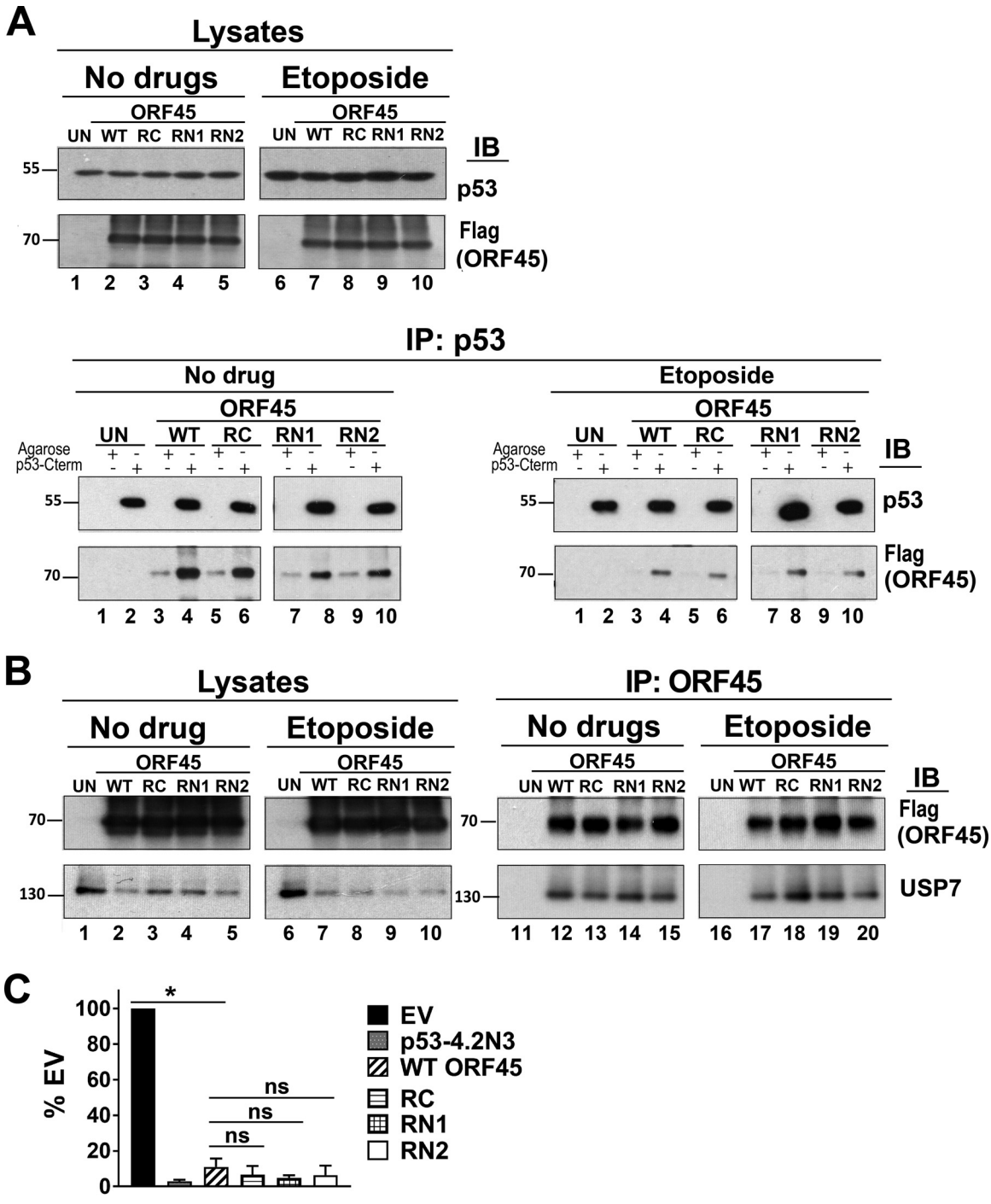

FIG 9 Subcellular localization of ORF45 does not affect its interactions with p53 and USP7, nor its ability to suppress p53-driven Luc expression. (A) ORF45 pulldown using p53-binding Ab. U2OS cells were transfected with plasmids expressing ORF45-Flag, ORF45^{RC}-Flag, ORF45^{RN1}-Flag, or ORF45^{RN2}-Flag or were left untransfected (UN). At 1 8 h p.t., the cells were stimulated with 10 μM etoposide for 6 h. p53 was immunoprecipitated with p53 C terminus-binding VHH Ab. Presence of wild-type or mutant ORF45-Flag fusions and p53 in the lysates and immunoprecipitants was tested with mouse α-Flag and mouse α-p53 DO7 Abs. (B) USP7 pulldown using Flag Ab binding to ORF45-Flag fusion proteins. U2OS cells were transfected with plasmids expressing ORF45-Flag, ORF45^{RC}-Flag, ORF45^{RN1}-Flag, or ORF45^{RN2}-Flag or were left untransfected (UN). Presence of USP7 and wild-type or mutant ORF45-Flag fusions in the lysates and immunoprecipitants was tested with rabbit α-USP7 and mouse α-Flag Abs. (C) p53-Luc assay for cells expressing ORF45 (wild type or the indicated mutants) stimulated with etoposide. U2OS cells were transfected with either p53-responsive reporter pGL13 and EV or with plasmids expressing *p53*R273, ORF45-Flag, ORF45^{RC}-Flag, ORF45^{RN1}-Flag, or ORF45^{RN2}-Flag. At 18 h posttransfection (p.t.), the cells were stimulated with 5 μM etoposide and then incubated for 24 h. Firefly luciferase levels were measured with the One-Glo luciferase assay system. *P* values were calculated using Student's *t* test ($n = 4$). ns, $P > 0.05$; **, $P \leq 0.001$.

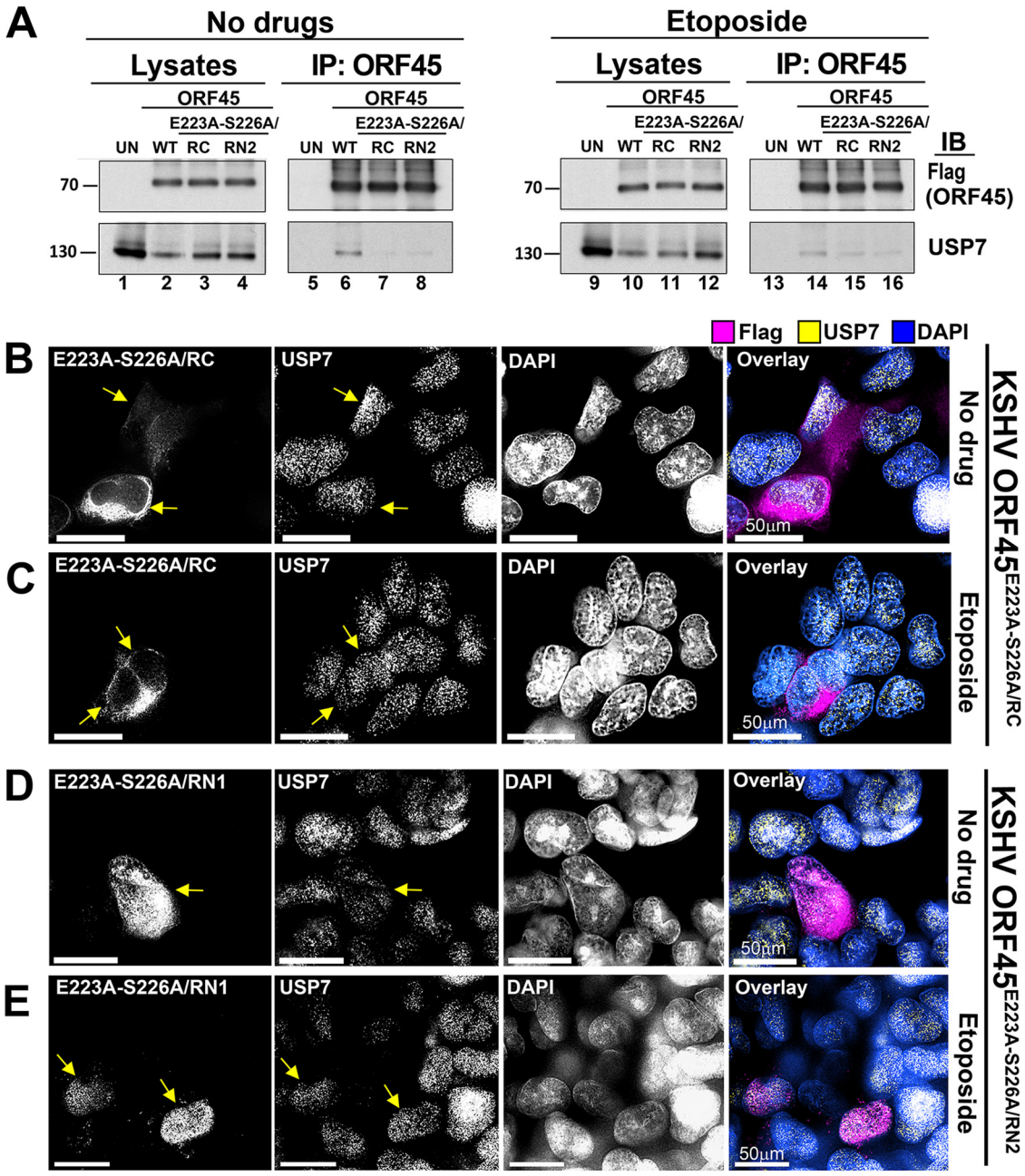

FIG 10 ORF45 double mutants lack USP7-binding activity and do not alter the subcellular localization of USP7. (A) USP7 pulldown using α-Flag Ab. U2OS cells were transfected with plasmids expressing ORF45-Flag, ORF45$^{E223A-S226A/RC}$-Flag, or ORF45$^{E223A-S226A/RN2}$-Flag or were left untransfected (UN). At 18 h p.t., the cells were stimulated with 10 μM etoposide for 6 h. ORF45-Flag fusion proteins were immunoprecipitated with α-Flag Ab. Presence of wild-type or mutant ORF45-Flag fusions and USP7 in the lysates and immunoprecipitated fractions was tested with mouse α-Flag and rabbit α-USP7 Abs. (B to E) Subcellular localization of USP7 in the presence of ORF45 double mutants. U2OS cells were transfected with plasmids expressing ORF45$^{E223A-S226A/RC}$-Flag or ORF45$^{E223A-S226A/RN2}$-Flag. At 18 h p.t., the cells were left untreated (A, C) or were stimulated with 10 μM etoposide for 1.5 h (B, D), fixed with methanol, and stained with the indicated Abs. The images were taken as Z-stack sections and subjected to digital deconvolution. Bar, 50 μm.

consequence of ORF45 modulating USP7 activity and some represent a new, direct interaction, as the ORF45$^{E223A-S226A}$ mutant, which no longer binds to USP7, still inhibited the transcriptional transactivation function of p53.

ORF45 shuttles extensively between the nucleus and the cytoplasm since ORF45 possesses NLS and NES motifs. Translocation between the nucleus and the cytoplasm is important for ORF45-USP7 cytoplasmic sequestration (26). Our experiments with

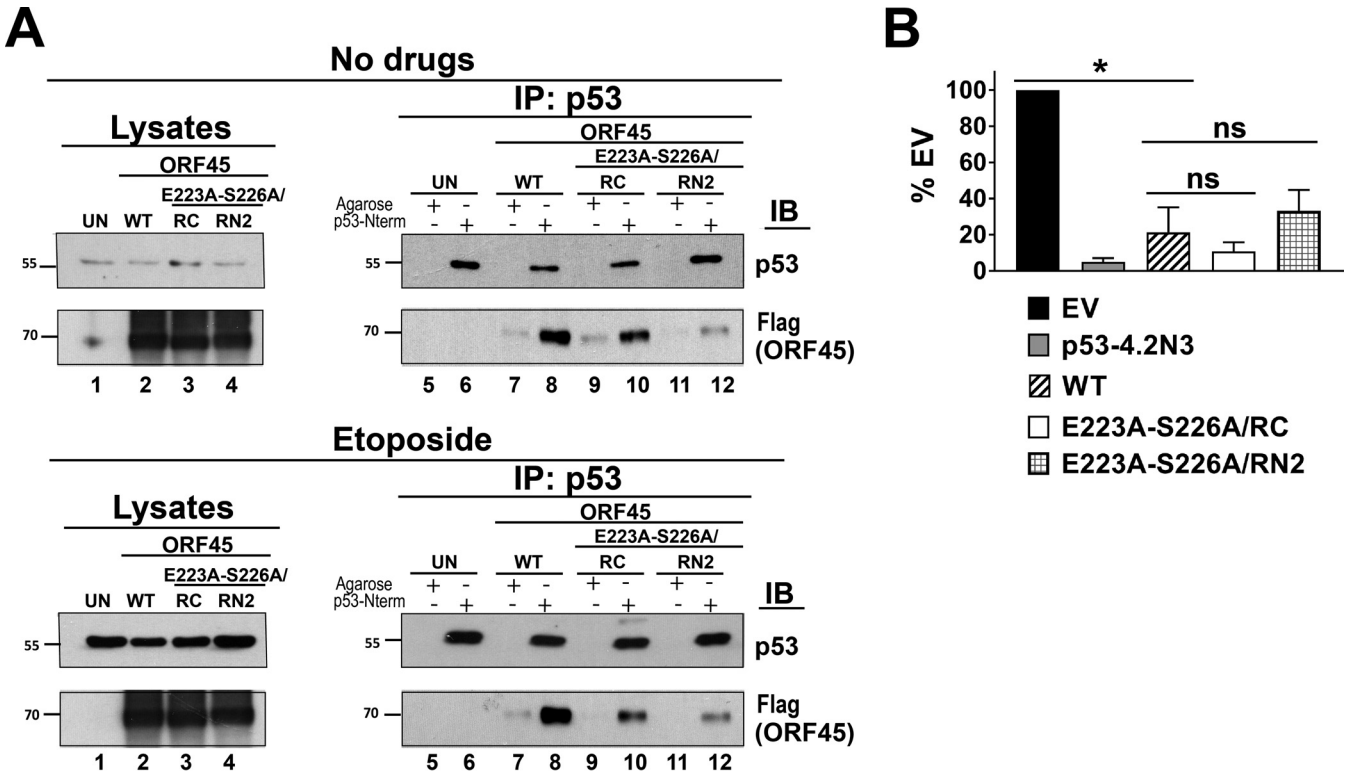

FIG 11 ORF45 double mutants bind to p53 and inhibit p53 transcriptional activity. (A) ORF45 pulldown using p53-binding Ab. U2OS cells were transfected with plasmids expressing ORF45-Flag, ORF45$^{E223A-S226A/RC}$-Flag, or ORF45$^{E223A-S226A/RN2}$-Flag or were left untransfected (UN). At 18 h p.t., the cells were stimulated with 10 μM etoposide for 6 h. p53 was immunoprecipitated with p53 C terminus-binding VHH Ab. Presence of wild-type or mutant ORF45-Flag fusions and p53 in the lysates and immunoprecipitants was tested with mouse α-Flag and mouse α-p53 DO7 Abs. (B) p53-Luc assay for cells expressing ORF45 (wild type or the indicated mutants) stimulated with etoposide. U2OS cells were transfected with either p53-responsive reporter pGL13 and EV or plasmids expressing *p53*R273, ORF45-Flag, ORF45$^{E223A-S226A/RC}$-Flag, or ORF45$^{E223A-S226A/RN2}$-Flag. At 18 h posttransfection (p.t.), the cells were stimulated with 5 μM etoposide and then incubated for 24 h. Firefly luciferase levels were measured with the One-Glo luciferase assay system. *P* values were calculated using Student's *t* test ($n = 4$). ns, $P > 0.05$; *, $P \leq 0.001$.

ORF45 mutants restricted to either the nucleus or the cytoplasm demonstrate that the shuttling of ORF45 is also required for cytoplasmic sequestration of p53.

Cytoplasmic sequestration of activated p53 and increased ubiquitination represent two different pathways by which ORF45 interferes with p53 function. Direct inhibition of p53 transactivation in the nucleus represent the third mode of inhibition, as the double mutant ORF45$^{E223A-S226A/RN2}$, which no longer binds USP7 and is nuclearly localized, nevertheless inhibited p53 transactivation. The details of this third mechanism of action are the subject of future studies.

One limitation of these experiments stems from the fact that ORF45 is an essential gene. An ORF45 deletion virus is not viable in KSHV, nor in murine herpesvirus virus 68 (MHV-68) (39, 46). Point mutations in ORF45 have been generated in the context of the viral genome that affect specific functions of the protein, such as nuclear localization or the ORF33 interaction domain (26). Similar studies are needed in the future. Such studies are not trivial, as most cell lines evolved to selectively change many p53 functions and since in the context of KSHV infection, other proteins, such as LANA, also impinge on p53 signaling.

Indeed, modulation of p53 has been described for multiple other KSHV-encoded proteins (4, 13–17, 19–22). This remarkable functional redundancy emphasizes the importance for the virus to counteract p53 during all stages of the viral life cycle (47–49): during latent genome persistence using LANA, vIRF-1, and vIRF-3 and during lytic replication using ORF45. The viral interference with p53 signaling would prevent premature p53-dependent apoptosis due to the DDR-sensing viral replication intermediates and recombination products.

TABLE 1 Primer sequences

Gene or primer name	Primer sequence
ORF45	
ORF45-5-EcoRI-F	5′-ATGAATTCGCCACCATGGCGATGTTTGTGAGGACCTCGTCTA-3′
ORF45-3Flag-NotI-R	5′-ATGCGGCCGCTCACTTGTCGTCGTCGTCCTTGTAGTCGATGTCGTGGTCCTTGTAGTCACCGTCGTGGTCCTTGTAGTCGTCCAGCCACGGCCAGTTATATGC-3′
ORF45-3Flag-XhoI-R	5′-ATCTCGACTCACTTGTCGTCGTCGTCCTTGTAGTCGATGTCGTGGTCCTTGTAGTCACCGTCGTGGTCCTTGTAGTCGTCCAGCCACGGCCAGTTATATGC-3′
ORF45$^{E223A-S226A}$	
ORF45-5-EcoRI-F	5′-ATGAATTCGCCACCATGGCGATGTTTGTGAGGACCTCGTCTA-3′
ORF45-E223A-S226A-R	5′-CAGGGGGCGCCACGCGGGCCCAGCATCAGGGTCGCTGTAT-3′
ORF45-E223A-S226A-F	5′-ATACAGCGACCCTGATGCTG GGCCCGCG TGGCGCCCCCTG-3′
ORF45-3Flag-NotI-R	5′-ATGCGGCCGCTCACTTGTCGTCGTCGTCCTTGTAGTCGATGTCGTGGTCCTTGTAGTCACCGTCGTGGTCCTTGTAGTCGTCCAGCCACGGCCAGTTATATGC-3′

[a]Nucleotide sequences for primers that were used to design ORF45-expressing constructs.

MATERIALS AND METHODS

Cell lines. U2OS human osteosarcoma cells were grown in Dulbecco's modified Eagle medium (DMEM; Gibco) supplemented with 10% fetal bovine serum (FBS) and 1% penicillin-streptomycin. The TREx BCBL1-RTA PEL-derived cell line was grown in RPMI supplemented with 10% tetracycline (Tet)-free FBS, 1% L-glutamine, 200 μg/ml hygromycin B, and 1% penicillin-streptomycin.

Plasmid constructs. pGL13, a firefly luciferase reporter plasmid containing 13 p53 binding elements, pCMV-Neo-Bam, and vectors expressing wild-type and dominant negative mutant p53 pCMV-Neo-Bam-p53WT and pCMV-Neo-Bam-*p53*R273H (pC53-*4.2N3*), respectively, were described elsewhere (50, 51). pGL3 control vector expressing firefly luciferase under SV40 promoter was purchased from Promega. pOME0016, referred to as pDEST47-ORF45-Flag, is described elsewhere (25). pCDN3.1-ORF45-Flag expressing wild-type ORF45 tagged with C-terminal 3×Flag (pDD2701) was generated by PCR amplification using primers described in Table S1 in the supplemental material and by subcloning into pCDNA3.1(+) vector using EcoRI-NotI sites. pCDNA3.1-ORF45$^{E223A-S226A}$-Flag (pDD2703) that expresses ORF45-Flag fusion harboring a mutation in the USP7 binding motif EGPS (amino acids 223 to 226) was constructed as follows. ORF45$^{E223A-S226A}$ was produced by splicing by overlap extension PCR (SOE-PCR) (43) using primers described in Table 1 and then cloned into pCDNA3.1(+) vector using EcoRI-NotI sites. pCDNA3.1-ORF45^{RN1}-Flag (pDD2708), pCDN3.1-ORF45^{RN2}-Flag (pDD2710), and pCDNA3.1-ORF45^{RC}-Flag (pDD2706) express ORF45-Flag fusions carrying mutations in NLS and NES motifs that were previously described (39). The mutant genes were tagged with the C-terminal Flag epitope by PCR amplification of ORF45 mutant sequences using primers listed for the wild-type ORF45 in Table 1 and subcloning into pCDNA3.1(+) vector using EcoRI-NotI sites. pCDNA3.1-ORF45$^{E223A-S226A/RC}$-Flag (pDD2711) was generated by cloning synthesized ORF45$^{E223A-S226A/RC}$-Flag fragment (Genewiz) into pCDNA3.1(+) vector at EcoRI-XhoI sites. ORF45$^{E223A-S226A/RN2}$-Flag (pDD2712) was generated by subcloning pCDNA3.1-ORF45$^{E223A-S226A}$-Flag EcoRI-SalI and pCDN3.1-ORF45^{RN2}-Flag SalI-NotI fragments into pCDNA3.1(+) vector.

Drugs and antibodies. Etoposide (catalog no. 02193918-CF; MP Biomedicals), nutlin-3 (catalog no. N6287; Millipore Sigma), MG132 (catalog no. 10012628; Cayman Chemicals), *N*-ethylmaleimide (NEM) (catalog no. E3876; Millipore Sigma), leptomycin B (LMB) (catalog no. L2913; Millipore Sigma), mouse α-Flag (M2, catalog no. F1804; Millipore Sigma), rabbit α-Flag (D6W5B, catalog no. 14793; Cell Signaling), mouse α-p53 pAb421 (catalog no. NBP2-62555; Novus Biologicals), mouse α-p53 (DO-7, catalog no. MA5-12557; Invitrogen), rabbit α-p53 pSer15 (catalog no. 9284; Cell Signaling), rabbit α-HAUSP (USP7) (D17C6, catalog no. 4833; Cell Signaling), mouse α-ATM (11G12, catalog no. 92356; Cell Signaling), rabbit α-ATM pSer1981 (D25E5, catalog no. 13050; Cell Signaling), mouse α-p21 (187, catalog no. sc-817; Santa-Cruz), mouse α-actin (catalog no. ab8226; Abcam), rabbit α-ubiquitin (catalog no. 3933; Cell Signaling), mouse α-ORF45 (2D4A5, catalog no. sc-53883; Santa-Cruz), mouse TrueBlot (catalog no. 18-8817-33; Rockland), horseradish peroxidase (HRP)-conjugated horse α-mouse (catalog no. PI-2000; Vector Laboratories), goat α-rabbit-HRP (catalog no. PI-1000; Vector Laboratories), horse α-mouse conjugated to fluorescein isothiocyanate (FITC) (catalog no. FI-2000; Vector Laboratories), goat α-rabbit Texas Red (catalog no. TI-1000; Vector Laboratories), VectaFluor Excel DyLight 488 α-mouse IgG (catalog no. DK-2488; Vector Laboratories), VectaFluor Excel DyLight 594 α-rabbit IgG (catalog no. DK-1594; Vector Laboratories), p53-N-term-Trap-A (epitope amino acids 1to 8, catalog no. pta-10; ChromoTek), p53-C-term-Trap-A (epitope amino acids 302 to 393, catalog no. pta2-10; ChromoTek), binding control (catalog no. bab-20; ChromoTek), and Protein A/G Plus-agarose (catalog no. sc-2003; Santa Cruz Biotechnology).

P53-Luc assay. U2OS cells were transfected with pGL13 and either pCMV-Neo-Bam, pCMV-Neo-Bam-*p53*R273H, or a vector expressing KSHV ORF45 wild type or mutant using Lipofectamine 2000. At 18 h post-transfection (p.t.), the cells were overlaid with fresh medium containing 5 μM etoposide or 10 μM nutlin-3 and incubated for an additional 24 h before measuring luciferase expression with the One-Glo luciferase assay system. Cell viability to determine cytotoxicity of each expressed ORF or the drug treatment was measured with the CellTiter-Glo luminescent cell viability assay (catalog no. G7570; Promega).

Coimmunoprecipitation. U2OS cells were transfected with a vector expressing KSHV ORF45 (wild type or mutant) using polyethylenimine (PEI) (linear, molecular weight 25,000, catalog no. 23966-1; Polysciences, Inc.) according to a previously described protocol with minor modifications (52). DNA-PEI solution was

prepared at a 1:3 ratio in Opti-MEM (catalog no. 31985062; Gibco) and incubated for 10 min at room temperature (RT) before adding it to the cells. At 18 h postinfection (p.i.), the cells were either stimulated with 10 μM etoposide or left untreated and then incubated for an additional 24 h. Harvested cells were lysed in 50 mM Tris (pH 7.4)-5mM ethylenediaminetetraacetic acid (EDTA)-0.5% Nonidet P-40 (NP-40)-150mM NaCl-5% sucrose (TENN) buffer supplemented with Complete protease inhibitor cocktail (Sigma-Aldrich) for 30 min on ice with occasional vortexing and spun down at 15,000 $\times$ *g* for 10 min. The lysates were precleared by incubation with protein A/G plus agarose beads (Santa Cruz Biotechnology) or "binding control" nonconjugated agarose beads (catalog no. bab-20; ChromoTek) and coimmunoprecipitated with either mouse α-Flag antibody and Protein A/G Plus-agarose beads or *p53-Trap N*-term_A and *p53-Trap* C-term_A (catalog no. pta-10 and pta2-10; ChromoTek), which are agarose-conjugated proteins specific for the p53 N or C terminus, respectively. The beads were washed with TENN buffer. Samples were precipitated with α-Flag Ab. The samples were analyzed by immunoblotting with the indicated Abs.

p53 Ubiquitination assay. U2OS cells transfected with a vector expressing an ORF of interest using PEI as described above were treated with 30 μM MG132 for 6 h and then incubated with 10 mM N-ethylmaleimide (NEM) for 10 min before harvesting. Samples were lysed in radioimmunoprecipitation (RIPA) buffer (50 mM Tris [pH 7.4] ,150mM NaCl-1% Triton X-100, 0.1% SDS, and 1% sodium deoxycholate) supplemented with 10 mM NEM, Benzonase nuclease (Sigma-Aldrich), and cOmplete protease inhibitor cocktail (Sigma-Aldrich) on ice for 30 min. The lysates were spun down at 15,000 $\times$ *g* for 10 min at 4°C, precleared with Protein A/G Plus-agarose beads for 30 min at 4°C, and immunoprecipitated by incubation with α-p53 pAb421 (18 h at 4°C) and Protein A/G Plus-agarose beads (1 h at 4°C). The samples were washed with radioimmunoprecipitation (RIPA) buffer and analyzed by immunoblotting with α-ubiquitin Ab and α-p53 DO7 Ab.

Cycloheximide chase. U2OS cells transfected with an expression vector for 24 h were stimulated with 10 μM etoposide for 1.5 h and then incubated with 100 μg/ml cycloheximide for the indicated times. The cells were lysed in RIPA buffer. Protein concentrations in lysates were normalized using a bicinchoninic acid (BCA) protein assay kit (catalog no. 23227; Thermo Scientific Pierce) and analyzed by SDS-PAGE and immunoblotting.

Immunoblotting. For protein accumulation assay, cells were lysed in RIPA buffer supplemented with benzonase nuclease and Complete protease inhibitor cocktail. Otherwise, the samples were prepared as indicated. The samples were separated by 6% or 12% SDS-PAGE, transferred to polyvinylidene fluoride (PVDF) membrane, blocked with 10% skim milk, and blotted with indicated Abs diluted either in 5% skim milk or 5% bovine serum albumin (BSA).

Immunofluorescence. The cells were plated onto coverslips and transfected with an expression vector. U2OS cells were transfected with PEI as described above. U87-MG and A549 cells and HUVEC cells were transfected with Lipofectamine LTX (catalog no. 15338100; Invitrogen) according to the manufacturer's protocol. At 18 h, the cells were stimulated with 10 μM etoposide for 1.5 to 2 h and fixed/permeabilized with ice-cold 100% methanol. Flag-conjugated proteins were stained with either mouse or rabbit α-Flag Ab and goat α-mouse or goat α-rabbit Ab conjugated to Texas Red or fluorescein isothiocyanate (FITC). Endogenously expressed cellular proteins were stained with one of the following Abs—mouse α-p53 DO7, rabbit α-p53 pSer15, mouse α-p21, or rabbit α-USP7)—and with either the VectaFluor Excel Amplified DyLight 594 anti-rabbit IgG kit or the VectaFluor Excel Amplified Dylight 488 anti-rabbit IgG kit (Vector Laboratories). The nuclei were stained with 4′,6-diamidino-2-phenylindole (DAPI). Z-stack images were collected using a DM4000B epifluorescence microscope (Leica) by setting the lowest and highest plane of the Z-axes and were subjected to deconvolution using Simple PCI_5 version 6.2 microscope software. The individual optical sections were exported as a multipage tag image file format (TIFF) file and processed using IMARIS version 7.1 software (Bitplane).

ACKNOWLEDGMENTS

This work was supported by Public Health Service (PHS) grants CA019014 and DE018304 to D.P.D. Core services at the UNC Lineberger comprehensive Cancer Center were supported by CA016086.

We thank Fanxiu Zhu (Department of Biological Science, Florida State University, Tallahassee, FL) for providing constructs expressing ORF45 RC, RN1, and RN2 mutants.

REFERENCES

1. Roy D, Sin SH, Damania B, Dittmer DP. 2011. Tumor suppressor genes FHIT and WWOX are deleted in primary effusion lymphoma (PEL) cell lines. Blood 118:e32-9–e39. https://doi.org/10.1182/blood-2010-12-323659.
2. Sarek G, Kurki S, Enback J, Iotzova G, Haas J, Laakkonen P, Laiho M, Ojala PM. 2007. Reactivation of the p53 pathway as a treatment modality for KSHV-induced lymphomas. J Clin Invest 117:1019–1028. https://doi.org/10.1172/JCI30945.
3. Petre CE, Sin SH, Dittmer DP. 2007. Functional p53 signaling in Kaposi's sarcoma-associated herpesvirus lymphomas: implications for therapy. J Virol 81:1912–1922. https://doi.org/10.1128/JVI.01757-06.
4. Friborg J, Kong W, Hottiger MO, Nabel GJ. 1999. p53 inhibition by the LANA protein of KSHV protects against cell death. Nature 402:889–894. https://doi.org/10.1038/47266.
5. Muñoz-Fontela C, Mandinova A, Aaronson SA, Lee SW. 2016. Emerging roles of p53 and other tumour-suppressor genes in immune regulation. Nat Rev Immunol 16:741–750. https://doi.org/10.1038/nri.2016.99.
6. Brooks CL, Gu W. 2006. p53 ubiquitination: Mdm2 and beyond. Mol Cell 21:307–315. https://doi.org/10.1016/j.molcel.2006.01.020.
7. Sheng Y, Saridakis V, Sarkari F, Duan S, Wu T, Arrowsmith CH, Frappier L. 2006. Molecular recognition of p53 and MDM2 by USP7/HAUSP. Nat Struct Mol Biol 13:285–291. https://doi.org/10.1038/nsmb1067.
8. Hu M, Gu L, Li M, Jeffrey PD, Gu W, Shi Y. 2006. Structural basis of competitive recognition of p53 and MDM2 by HAUSP/USP7: implications for the regulation of the p53-MDM2 pathway. PLoS Biol 4:e27. https://doi.org/10.1371/journal.pbio.0040027.

9. Tang J, Qu LK, Zhang J, Wang W, Michaelson JS, Degenhardt YY, El-Deiry WS, Yang X. 2006. Critical role for Daxx in regulating Mdm2. Nat Cell Biol 8:855–862. https://doi.org/10.1038/ncb1442.
10. Khoronenkova SV, Dianova II, Ternette N, Kessler BM, Parsons JL, Dianov GL. 2012. ATM-dependent downregulation of USP7/HAUSP by PPM1G activates p53 response to DNA damage. Mol Cell 45:801–813. https://doi.org/10.1016/j.molcel.2012.01.021.
11. Ireland-Gill A, Espina BM, Akil B, Gill PS. 1992. Treatment of acquired immunodeficiency syndrome-related Kaposi's sarcoma using bleomycin-containing combination chemotherapy regimens. Semin Oncol 19:32–37.
12. Gill PS, Wernz J, Scadden DT, Cohen P, Mukwaya GM, von Roenn JH, Jacobs M, Kempin S, Silverberg I, Gonzales G, Rarick MU, Myers AM, Shepherd F, Sawka C, Pike MC, Ross ME. 1996. Randomized phase III trial of liposomal daunorubicin versus doxorubicin, bleomycin, and vincristine in AIDS-related Kaposi's sarcoma. J Clin Oncol 14:2353–2364. https://doi.org/10.1200/JCO.1996.14.8.2353.
13. Chen W, Hilton IB, Staudt MR, Burd CE, Dittmer DP. 2010. Distinct p53, p53:LANA, and LANA complexes in Kaposi's sarcoma-associated herpesvirus lymphomas. J Virol 84:3898–3908. https://doi.org/10.1128/JVI.01321-09.
14. Shin YC, Nakamura H, Liang X, Feng P, Chang H, Kowalik TF, Jung JU. 2006. Inhibition of the ATM/p53 signal transduction pathway by Kaposi's sarcoma-associated herpesvirus interferon regulatory factor 1. J Virol 80:2257–2266. https://doi.org/10.1128/JVI.80.5.2257-2266.2006.
15. Baresova P, Musilova J, Pitha PM, Lubyova B. 2014. p53 tumor suppressor protein stability and transcriptional activity are targeted by Kaposi's sarcoma-associated herpesvirus-encoded viral interferon regulatory factor 3. Mol Cell Biol 34:386–399. https://doi.org/10.1128/MCB.01011-13.
16. Nakamura H, Li M, Zarycki J, Jung JU. 2001. Inhibition of p53 tumor suppressor by viral interferon regulatory factor. J Virol 75:7572–7582. https://doi.org/10.1128/JVI.75.16.7572-7582.2001.
17. Seo T, Park J, Lee D, Hwang SG, Choe J. 2001. Viral interferon regulatory factor 1 of Kaposi's sarcoma-associated herpesvirus binds to p53 and represses p53-dependent transcription and apoptosis. J Virol 75:6193–6198. https://doi.org/10.1128/JVI.75.13.6193-6198.2001.
18. Lee HR, Toth Z, Shin YC, Lee JS, Chang H, Gu W, Oh TK, Kim MH, Jung JU. 2009. Kaposi's sarcoma-associated herpesvirus viral interferon regulatory factor 4 targets MDM2 to deregulate the p53 tumor suppressor pathway. J Virol 83:6739–6747. https://doi.org/10.1128/JVI.02353-08.
19. Jäger W, Santag S, Weidner-Glunde M, Gellermann E, Kati S, Pietrek M, Viejo-Borbolla A, Schulz TF. 2012. The ubiquitin-specific protease USP7 modulates the replication of Kaposi's sarcoma-associated herpesvirus latent episomal DNA. J Virol 86:6745–6757. https://doi.org/10.1128/JVI.06840-11.
20. Chavoshi S, Egorova O, Lacdao IK, Farhadi S, Sheng Y, Saridakis V. 2016. Identification of Kaposi sarcoma herpesvirus (KSHV) vIRF1 protein as a novel interaction partner of human deubiquitinase USP7. J Biol Chem 291:6281–6291. https://doi.org/10.1074/jbc.M115.710632.
21. Xiang Q, Ju H, Li Q, Mei SC, Chen D, Choi YB, Nicholas J. 2018. Human herpesvirus 8 interferon regulatory factors 1 and 3 mediate replication and latency activities via interactions with USP7 deubiquitinase. J Virol 92. https://doi.org/10.1128/JVI.02003-17.
22. Lee HR, Choi WC, Lee S, Hwang J, Hwang E, Guchhait K, Haas J, Toth Z, Jeon YH, Oh TK, Kim MH, Jung JU. 2011. Bilateral inhibition of HAUSP deubiquitinase by a viral interferon regulatory factor protein. Nat Struct Mol Biol 18:1336–1344. https://doi.org/10.1038/nsmb.2142.
23. Nakamura H, Lu M, Gwack Y, Souvlis J, Zeichner SL, Jung JU. 2003. Global changes in Kaposi's sarcoma-associated virus gene expression patterns following expression of a tetracycline-inducible Rta transactivator. J Virol 77:4205–4220. https://doi.org/10.1128/jvi.77.7.4205-4220.2003.
24. Ueda K, Ishikawa K, Nishimura K, Sakakibara S, Do E, Yamanishi K. 2002. Kaposi's sarcoma-associated herpesvirus (human herpesvirus 8) replication and transcription factor activates the K9 (vIRF) gene through two distinct *cis* elements by a non-DNA-binding mechanism. J Virol 76:12044–12054. https://doi.org/10.1128/jvi.76.23.12044-12054.2002.
25. Alzhanova D, Corcoran K, Bailey AG, Long K, Taft-Benz S, Graham RL, Broussard GS, Heise M, Neumann G, Halfmann P, Kawaoka Y, Baric RS, Damania B, Dittmer DP. 2021. Novel modulators of p53-signaling encoded by unknown genes of emerging viruses. PLoS Pathog 17:e1009033. https://doi.org/10.1371/journal.ppat.1009033.
26. Gillen J, Li W, Liang Q, Avey D, Wu J, Wu F, Myoung J, Zhu F. 2015. A survey of the interactome of Kaposi's sarcoma-associated herpesvirus ORF45 revealed its binding to viral ORF33 and cellular USP7, resulting in stabilization of ORF33 that is required for production of progeny viruses. J Virol 89:4918–4931. https://doi.org/10.1128/JVI.02925-14.
27. Dittmer D, Pati S, Zambetti G, Chu S, Teresky AK, Moore M, Finlay C, Levine AJ. 1993. Gain of function mutations in p53. Nat Genet 4:42–46. https://doi.org/10.1038/ng0593-42.
28. Finlay CA, Hinds PW, Levine AJ. 1989. The p53 proto-oncogene can act as a suppressor of transformation. Cell 57:1083–1093. https://doi.org/10.1016/0092-8674(89)90045-7.
29. Vassilev LT, Vu BT, Graves B, Carvajal D, Podlaski F, Filipovic Z, Kong N, Kammlott U, Lukacs C, Klein C, Fotouhi N, Liu EA. 2004. *In vivo* activation of the p53 pathway by small-molecule antagonists of MDM2. Science 303:844–848. https://doi.org/10.1126/science.1092472.
30. Kamaraj B, Bogaerts A. 2015. Structure and function of p53-DNA complexes with inactivation and rescue mutations: a molecular dynamics simulation study. PLoS One 10:e0134638. https://doi.org/10.1371/journal.pone.0134638.
31. Kitayner M, Rozenberg H, Kessler N, Rabinovich D, Shaulov L, Haran TE, Shakked Z. 2006. Structural basis of DNA recognition by p53 tetramers. Mol Cell 22:741–753. https://doi.org/10.1016/j.molcel.2006.05.015.
32. Chandar N, Billig B, McMaster J, Novak J. 1992. Inactivation of p53 gene in human and murine osteosarcoma cells. Br J Cancer 65:208–214. https://doi.org/10.1038/bjc.1992.43.
33. Holowaty MN, Zeghouf M, Wu H, Tellam J, Athanasopoulos V, Greenblatt J, Frappier L. 2003. Protein profiling with Epstein-Barr nuclear antigen-1 reveals an interaction with the herpesvirus-associated ubiquitin-specific protease HAUSP/USP7. J Biol Chem 278:29987–29994. https://doi.org/10.1074/jbc.M303977200.
34. Saito S, Yamaguchi H, Higashimoto Y, Chao C, Xu Y, Fornace AJ, Appella E, Anderson CW. 2003. Phosphorylation site interdependence of human p53 post-translational modifications in response to stress. J Biol Chem 278:37536–37544. https://doi.org/10.1074/jbc.M305135200.
35. Al Rashid ST, Dellaire G, Cuddihy A, Jalali F, Vaid M, Coackley C, Folkard M, Xu Y, Chen BP, Chen DJ, Lilge L, Prise KM, Bazett Jones DP, Bristow RG. 2005. Evidence for the direct binding of phosphorylated p53 to sites of DNA breaks *in vivo*. Cancer Res 65:10810–10821. https://doi.org/10.1158/0008-5472.CAN-05-0729.
36. Zhu FX, Yuan Y. 2003. The ORF45 protein of Kaposi's sarcoma-associated herpesvirus is associated with purified virions. J Virol 77:4221–4230. https://doi.org/10.1128/jvi.77.7.4221-4230.2003.
37. Momand J, Zambetti GP, Olson DC, George D, Levine AJ. 1992. The *mdm-2* oncogene product forms a complex with the p53 protein and inhibits p53-mediated transactivation. Cell 69:1237–1245. https://doi.org/10.1016/0092-8674(92)90644-r.
38. Renne R, Zhong W, Herndier B, McGrath M, Abbey N, Kedes D, Ganem D. 1996. Lytic growth of Kaposi's sarcoma-associated herpesvirus (human herpesvirus 8) in culture. Nat Med 2:342–346. https://doi.org/10.1038/nm0396-342.
39. Li X, Zhu F. 2009. Identification of the nuclear export and adjacent nuclear localization signals for ORF45 of Kaposi's sarcoma-associated herpesvirus. J Virol 83:2531–2539. https://doi.org/10.1128/JVI.02209-08.
40. Karijolich J, Zhao Y, Peterson B, Zhou Q, Glaunsinger B. 2014. Kaposi's sarcoma-associated herpesvirus ORF45 mediates transcriptional activation of the HIV-1 long terminal repeat via RSK2. J Virol 88:7024–7035. https://doi.org/10.1128/JVI.00931-14.
41. Kuang E, Fu B, Liang Q, Myoung J, Zhu F. 2011. Phosphorylation of eukaryotic translation initiation factor 4B (EIF4B) by open reading frame 45/p90 ribosomal S6 kinase (ORF45/RSK) signaling axis facilitates protein translation during Kaposi sarcoma-associated herpesvirus (KSHV) lytic replication. J Biol Chem 286:41171–41182. https://doi.org/10.1074/jbc.M111.280982.
42. Zhu FX, King SM, Smith EJ, Levy DE, Yuan Y. 2002. A Kaposi's sarcoma-associated herpesviral protein inhibits virus-mediated induction of type I interferon by blocking IRF-7 phosphorylation and nuclear accumulation. Proc Natl Acad Sci U S A 99:5573–5578. https://doi.org/10.1073/pnas.082420599.
43. Kuang E, Tang Q, Maul GG, Zhu F. 2008. Activation of p90 ribosomal S6 kinase by ORF45 of Kaposi's sarcoma-associated herpesvirus and its role in viral lytic replication. J Virol 82:1838–1850. https://doi.org/10.1128/JVI.02119-07.
44. Avey D, Tepper S, Li W, Turpin Z, Zhu F. 2015. Phosphoproteomic analysis of KSHV-infected cells reveals roles of ORF45-activated RSK during lytic replication. PLoS Pathog 11:e1004993. https://doi.org/10.1371/journal.ppat.1004993.

45. Sathish N, Zhu FX, Yuan Y. 2009. Kaposi's sarcoma-associated herpesvirus ORF45 interacts with kinesin-2 transporting viral capsid-tegument complexes along microtubules. PLoS Pathog 5:e1000332. https://doi.org/10.1371/journal.ppat.1000332.
46. Jia X, Shen S, Lv Y, Zhang Z, Guo H, Deng H. 2016. Tegument protein ORF45 plays an essential role in virion morphogenesis of murine gammaherpesvirus 68. J Virol 90:7587–7592. https://doi.org/10.1128/JVI.03231-15.
47. Cesarman E, Damania B, Krown SE, Martin J, Bower M, Whitby D. 2019. Kaposi sarcoma. Nat Rev Dis Primers 5:9. https://doi.org/10.1038/s41572-019-0060-9.
48. Broussard G, Damania B. 2019. KSHV: immune modulation and immunotherapy. Front Immunol 10:3084. https://doi.org/10.3389/fimmu.2019.03084.
49. Lee HR, Brulois K, Wong L, Jung JU. 2012. Modulation of immune system by Kaposi's sarcoma-associated herpesvirus: lessons from viral evasion strategies. Front Microbiol 3:44.
50. Baker SJ, Markowitz S, Fearon ER, Willson JK, Vogelstein B. 1990. Suppression of human colorectal carcinoma cell growth by wild-type p53. Science 249:912–915. https://doi.org/10.1126/science.2144057.
51. Kern SE, Pietenpol JA, Thiagalingam S, Seymour A, Kinzler KW, Vogelstein B. 1992. Oncogenic forms of p53 inhibit p53-regulated gene expression. Science 256:827–830. https://doi.org/10.1126/science.1589764.
52. Durocher Y, Perret S, Kamen A. 2002. High-level and high-throughput recombinant protein production by transient transfection of suspension-growing human 293-EBNA1 cells. Nucleic Acids Res 30:E9. https://doi.org/10.1093/nar/30.2.e9.